Mol Neurobiol (2017) 54:3859–3878
DOI 10.1007/s12035-016-0010-4

Genome-wide Analysis of RARβ Transcriptional Targets in Mouse Striatum Links Retinoic Acid Signaling with Huntington's Disease and Other Neurodegenerative Disorders

Anna Niewiadomska-Cimicka[1,2,3,4,5] · **Agnieszka Krzyżosiak**[1,2,3,4,5,6] · **Tao Ye**[1,2,3,4] · **Anna Podleśny-Drabiniok**[1,2,3,4,5] · **Doulaye Dembélé**[1,2,3,4] · **Pascal Dollé**[1,2,3,4,5] · **Wojciech Krężel**[1,2,3,4,5]

Received: 13 December 2015 / Accepted: 8 June 2016 / Published online: 12 July 2016

Abstract Retinoic acid (RA) signaling through retinoic acid receptors (RARs), known for its multiple developmental functions, emerged more recently as an important regulator of adult brain physiology. How RAR-mediated regulation is achieved is poorly known, partly due to the paucity of information on critical target genes in the brain. Also, it is not clear how reduced RA signaling may contribute to pathophysiology of diverse neuropsychiatric disorders. We report the first genome-wide analysis of RAR transcriptional targets in the brain. Using chromatin immunoprecipitation followed by high-throughput sequencing and transcriptomic analysis of RARβ-null mutant mice, we identified genomic targets of RARβ in the striatum. Characterization of RARβ transcriptional targets in the mouse striatum points to mechanisms through which RAR may control brain functions and display neuroprotective activity. Namely, our data indicate with statistical significance (FDR 0.1) a strong contribution of RARβ in controlling neurotransmission, energy metabolism, and transcription, with a particular involvement of G-protein coupled receptor ($p = 5.0e^{-5}$), cAMP ($p = 4.5e^{-4}$), and calcium signaling ($p = 3.4e^{-3}$). Many identified RARβ target genes related to these pathways have been implicated in Alzheimer's, Parkinson's, and Huntington's disease (HD), raising the possibility that compromised RA signaling in the striatum may be a mechanistic link explaining the similar affective and cognitive symptoms in these diseases. The RARβ transcriptional targets were particularly enriched for transcripts affected in HD. Using the R6/2 transgenic mouse model of HD, we show that partial sequestration of RARβ in huntingtin protein aggregates may account for reduced RA signaling reported in HD.

Keywords Retinoic acid · RAR · Huntington's disease · Striatum · Nucleus accumbens · Response elements · ChIP-seq · Transcriptome

Electronic supplementary material The online version of this article (doi:10.1007/s12035-016-0010-4) contains supplementary material, which is available to authorized users.

✉ Wojciech Krężel
krezel@igbmc.fr

[1] Institut de Génétique et de Biologie Moléculaire et Cellulaire, 1 rue Laurent Fries, 67404 Illkirch Cedex, France

[2] Centre National de la Recherche Scientifique, UMR 7104 Illkirch, France

[3] Institut National de la Santé et de la Recherche Médicale, U 964 Illkirch, France

[4] Université de Strasbourg, Illkirch, France

[5] Fédération de Médecine Translationnelle de Strasbourg (FMTS), Strasbourg, France

[6] Present address: MRC Laboratory of Molecular Biology, Francis Crick Avenue, CB2 0QH Cambridge, UK

Introduction

Over the last decade, retinoic acid (RA), a bioactive metabolite of vitamin A, emerged as an important regulator of brain development and functions. Signaling by RA is mediated by its binding to nuclear receptors (RARα, β, γ), which form heterodimers with retinoid X receptors (RXRα, β, γ) and act as ligand-controlled transcription factors. Several lines of evidence indicate that RA signaling is particularly important for functions of the striatum, the brain region critically involved in control of several functions including motor control, cognition, reward,

and motivation. Accordingly, among different brain regions, the adult rodent striatum contains some of the highest levels of RA [1]. The striatum is also a site of strong expression of two retinoid receptors, RARβ and RXRγ [2, 3]. Genetic ablation of RARβ and/or RXRγ leads to abnormal striatal functions, revealed by deficits in motor coordination and depressive-like behaviors [4, 5]. Whereas some of these phenotypic abnormalities may have a developmental origin ([6, 7]), post-natal functions of these receptors have also been documented on evidence of RXRγ-dependent control of affective behaviors and dopamine D2 receptor (DRD2) signaling in the nucleus accumbens shell (NAcSh) [5, 8]. Despite these studies, our understanding of RA-dependent control of striatal functions is limited, due to the scarcity of knowledge about the transcriptional targets of RA signaling in the brain, which until now were mostly suggested by in vitro studies performed on different types of cultured cells and for few genes also validated in selected brain regions (for review see [9, 10]). To date, the best characterized RA-targets are the RARβ (*Rarb*) gene itself [11, 12] and the dopamine D2 receptor (*Drd2*) gene [4, 13].

Identification of mechanisms of RA signaling in the striatum should have direct relevance for understanding of pathophysiology of Huntington's disease (HD), Parkinson's disease (PD), schizophrenia, or depression, which are all associated with striatal dysfunction [14]. Importantly, compromised RA signaling due to reduced expression or activity of RA-synthesizing enzymes was documented for retinaldehyde dehydrogenase (RALDH) 1 in PD [15] or RALDH2 in Alzheimer's disease (AD) [16–18]. A causal relationship between compromised RALDH1 or RALDH2 activity and these diseases has also been suggested [16, 19]. Reduced expression of retinoid receptors in the striatum was reported in HD, a disease which severely affects striatal functions and is caused by expansion of polyglutamine repeats in the huntingtin (HTT) protein, leading to abnormal HTT aggregates. Specifically, reduced RARβ and RXRγ transcript levels were observed in the striatum from HD patients [20], whereas in the R6/2 transgenic mouse model of HD only a reduction of RXRγ mRNA was reported [21]. It is therefore tempting to hypothesize that an overall reduction of RA bioavailability or reduced expression and signaling of RARs in the striatum may constitute a mechanistic link between common symptoms of HD, PD, and AD, which all eventually show atrophy or neurodegeneration of ventral striatum and associated psychiatric symptoms.

We report here the first genome-wide analysis of RAR targets in the brain. Through genome-wide mapping of RARβ binding sites in the striatum enriched for ventral region and determination of transcriptome changes occurring in the ventral striatum (nucleus accumbens shell; NAcSh) after genetic ablation of RARβ, we distinguish bona fide (genes bearing RARβ binding sites, which expression is changed in RARβ$^{-/-}$ NAcSh), potential (genes bearing RARβ binding sites, but which expression is unchanged in RARβ$^{-/-}$ NAcSh), and presumably indirect targets (with altered expression in RARβ$^{-/-}$ NAcSh, but without RARβ binding sites) of RARβ. Functional annotations of those genes reveal exceptionally high links between compromised RA signaling and HD, and point to deficient signaling through G-protein coupled receptors (GPCRs), cAMP, and Ca^{2+} as a molecular link between compromised RARβ expression and some common histopathological and clinical symptoms of HD, PD, and AD. In support of this hypothesis, we found that ventral striatum, the region affected in all of these pathologies, is particularly prone to deficits in RA signaling. We also provide evidence that reduced RARβ expression in HD may result from partial sequestration of RARβ in aggregates of mutant HTT protein, which we characterized in the striatum of R6/2 transgenic mice.

Results

Genome-wide Identification of RARβ Binding Sites in Mouse Striatum Reveals Its Potential Transcriptional Targets and Suggests Implication of Retinoid Signaling in Neurological Disorders

To gain insight into transcriptional regulations by RARβ in the brain, we first investigated genome-wide distribution of RARβ binding sites in mouse striatum. For this purpose, we set-up conditions for efficient chromatin immunoprecipitation (ChIP) using striatum enriched for its ventral part. To test the specificity of ChIP, we performed a series of ChIP-qPCR analyses of a DNA region containing a known RA-response element (RARE) within the promoter of the RARβ gene [11, 12]. Accordingly, we demonstrated high (14-fold) enrichment of this region when compared to DNA region not containing RARβ binding sites [22], located -1203 to -1059 base pairs (bp) upstream of the RARβ transcription start site (TSS) [22] (Fig. 1a, left panel). Similarly, a 10-fold enrichment of RARE-containing region was observed after using anti-RARβ antibody as compared to a non-specific antibody directed against GFP (Fig. 1a, compare left and middle panels). The RARE-containing region was also highly enriched for histone 3 lysine 4 trimethylation (H3K4me3; Fig. 1a), which is associated with transcriptionally active or poised genes.

Using the same biological material, we then performed ChIP followed by high-throughput sequencing (ChIP-seq), which revealed 8075 RARβ binding sites when compared to ChIP-seq with anti-GFP antibody used as a negative control. Using the GPAT software [23], these binding sites were annotated to 5466 Ensembl transcripts, which corresponded to 4607 genes. As expected, among binding sites determined by ChIP-seq analysis we found the known RARE within the RARβ gene promoter (Fig. 1b). Functional annotations

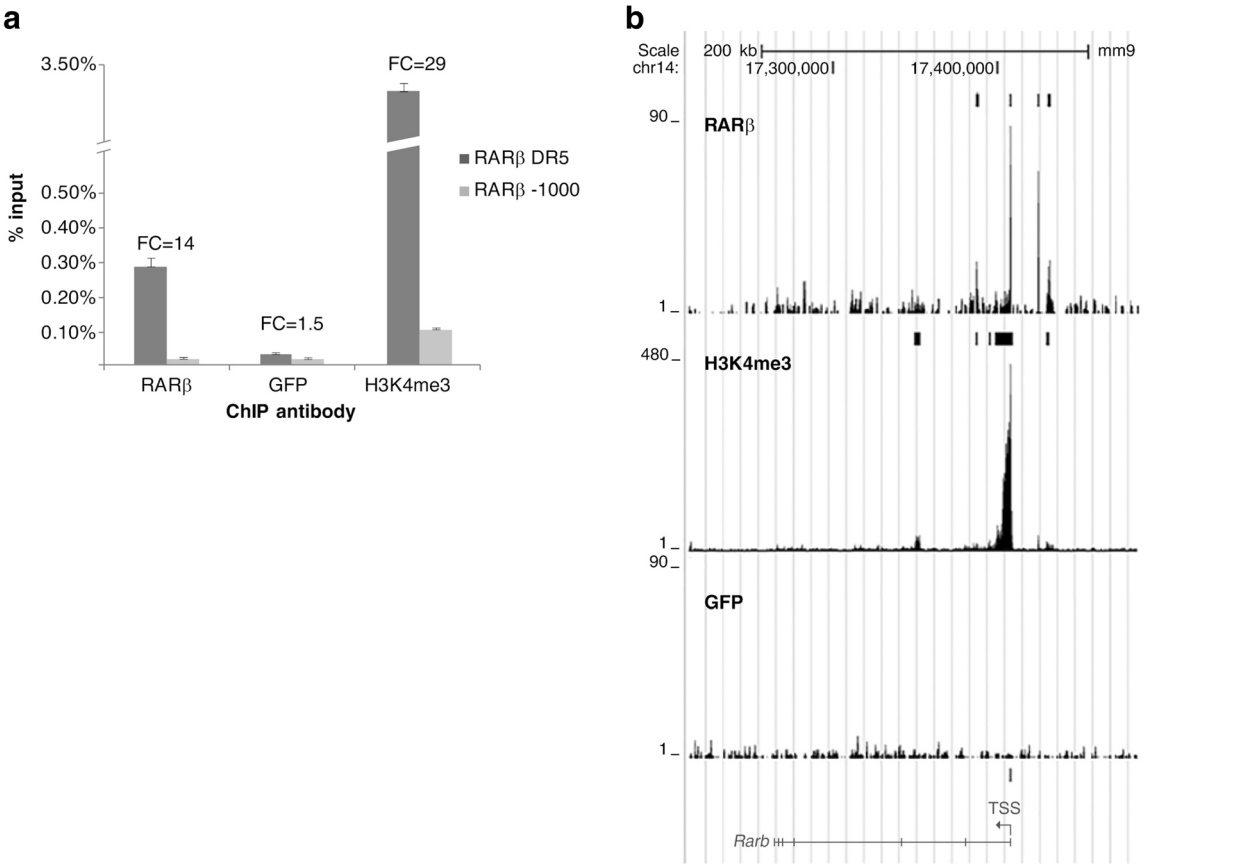

Fig. 1 Validation of RARβ ChIP and ChIP-seq data for the mouse striatum. **a** Quantification (qPCR amplification) of ChIP fragments of the region of the RARβ gene promoter containing a "direct repeat 5" (DR5) RARE (RARβ DR5, *black bars*) and another, far-upstream region (RARβ -1000; *gray bars*). *FC*, fold change. **b** University of California at Santa Cruz (UCSC) web browser view of sequence tag density in.wig file format of the RARβ- and H3K4me3-occupied sites of the RARβ gene locus. Sequence tag density of GFP used as negative control is also shown

carried out with the Database for Annotation, Visualization, and Integrated Discovery (DAVID) [24] and Genomic Regions Enrichment of Annotations Tool (GREAT) [25] pointed to protein modifications, intracellular signaling cascades, regulation of small GTPase-mediated signal transduction, synaptic transmission/neurotransmitter release, cytoskeleton organization, and cell motility ($p = 10e^{-14}$–$10e^{-5}$), as the main biological processes associated with genes bearing RARβ binding sites. When analyzed using Ingenuity Pathway Analysis (IPA), such potential RARβ target genes revealed remarkably high association with neurological diseases including, by order of statistical significance, Huntington's disease ($p = 1.15e^{-28}$), schizophrenia ($p = 1.09e^{-14}$), AD ($p = 1.87e^{-7}$), and PD ($p = 8.32e^{-7}$). Interestingly, both IPA and DAVID analyses revealed that 287 genes bearing RARβ binding sites were associated with HD. These genes (Table 1, Supplementary Table S1) are primarily involved in control of mitochondrial functions including oxidative phosphorylation, e.g., different subunits of ATP synthase, cytochrome c oxidases (*Cox*), NADH dehydrogenase, succinate dehydrogenase complex subunits (*Sdha* and *Sdhc*), and general mitochondrial functions controlled for example by voltage-dependent anion channels (*Vdac 1–2*). This suggests that abnormal mitochondrial functions under conditions of altered RARβ signaling may underlie common aspects of different neurodegenerative diseases. Accordingly, 64 out of 287 genes associated with HD were also reported to play a role in AD and/or PD pathophysiology (Supplementary Table S1). However, the majority of genes (223 genes) bearing RARβ binding sites were associated exclusively with HD, and not with AD or PD. Those genes are strongly linked to transcriptional regulation (52 genes, see Supplementary Table S2) and include two subunits of RNA polymerase II (*Polr2a*, *Polr2i*), transcription factors (e.g., *Meis2*, *Sp1*, *Notch2*, *Foxp1*, *Nr1d1*), and cofactors (e.g., *Ppargc1b*, *Rcor1*), or chromatin-modifying enzymes (e.g., *Hdac2*, *Kdm3a*). Furthermore, this "HD-specific" pool of genes was also enriched for GPCRs (e.g., dopaminergic receptors *Drd1*, *Drd2*, *Drd3*, cannabinoid receptor *Cnr1*, or cholinergic receptors *Chrm1*, *Chrm4*) and proteins involved in GPCR signal transduction, including components of the cAMP signaling pathway or linked to calcium signaling (Table 1, Supplementary Table S1). Abnormal functions of these signaling pathways may be relevant for psychiatric symptoms,

Table 1 Top 10 pathways (IPA analysis) related to genes containing at least one RARβ binding site and reported to be affected in HD

Pathways	*p* value	Genes
Oxidative phosphorylation	$2.59e^{-08}$	*Atp5a1*, *Atp5b*, *Atp5f1*, *Atp5g2*, *Atp5j*, *Cox4i1*, *Cox5a*, *Cox7a2l*, *Cox8b*, *Ndufa13*, *Ndufa2*, *Ndufa3*, *Ndufa5*, *Ndufb2*, *Ndufb4*, *Ndufb5*, *Ndufb7*, *Ndufb8*, *Ndufs6*, *Ndufs7*, *Ndufs8*, *Sdha*, *Sdhc*, *Uqcrb*, *Uqcrc1*, *Uqcrc2*, *Uqcrq*
Mitochondrial dysfunction	$9.68e^{-08}$	*Atp5a1*, *Atp5b*, *Atp5f1*, *Atp5g2*, *Atp5j*, *Cox4i1*, *Cox5a*, *Cox7a2l*, *Cox8b*, *Ndufa13*, *Ndufa2*, *Ndufa3*, *Ndufa4l2*, *Ndufa5*, *Ndufb2*, *Ndufb4*, *Ndufb5*, *Ndufb7*, *Ndufb8*, *Ndufs6*, *Ndufs7*, *Ndufs8*, *Sdha*, *Sdhc*, *Uqcrb*, *Uqcrc1*, *Uqcrc2*, *Uqcrq*, *Vdac1*, *Vdac2*
G-Protein coupled receptor signaling	$4.96e^{-05}$	*Adcy5*, *Adora2a*, *Adrb1*, *Camk2a*, *Camk2b*, *Camk4*, *Chrm1*, *Chrm4*, *Cnr1*, *Drd1*, *Drd2*, *Gnal*, *Gnao1*, *Grm5*, *Htr1b*, *Htr6*, *Nfkb1*, *Pde10a*, *Pde1b*, *Plcb1*, *Plcb2*, *Plcb3*, *Prkcb*, *Ptk2b*, *Rap1gap*, *Rgs4*
CREB signaling in neurons	$2.13e^{-04}$	*Adcy5*, *Camk2a*, *Camk2b*, *Camk4*, *Gnal*, *Gnao1*, *Gnb5*, *Gng7*, *Grik2*, *Grin1*, *Grin2a*, *Grin2b*, *Grm5*, *Itpr1*, *Plcb1*, *Plcb2*, *Plcb3*, *Polr2a*, *Polr2i*, *Prkcb*
Neuropathic pain signaling in dorsal horn neurons	$2.44e^{-04}$	*Camk2a*, *Camk2b*, *Camk4*, *Grin1*, *Grin2a*, *Grin2b*, *Grm5*, *Itpr1*, *Kcnn3*, *Kcnq2*, *Ntrk2*, *Plcb1*, *Plcb2*, *Plcb3*, *Prkcb*, *Tac1*
cAMP-mediated signaling, including dopamine-DARPP32 feedback in cAMP signaling	$4.56e^{-04}$	*Adcy5*, *Adora2a*, *Adrb1*, *Camk2a*, *Camk2b*, *Camk4*, *Chrm1*, *Chrm4*, *Cnr1*, *Drd1*, *Drd2*, *Gnal*, *Gnao1*, *Htr1b*, *Htr6*, *Pde10a*, *Pde1b*, *Pkia*, *Ppp3ca*, *Rap1gap*, *Rgs4*
	$1.15e^{-03}$	*Adcy5*, *Atp2a2*, *Camk4*, *Drd1*, *Drd2*, *Grin1*, *Grin2a*, *Grin2b*, *Itpr1*, *Kcnj4*, *Nos1*, *Plcb1*, *Plcb2*, *Plcb3*, *Ppp1r1b*, *Ppp3ca*, *Prkcb*
Synaptic long-term potentiation	$2.32e^{-03}$	*Camk2a*, *Camk2b*, *Camk4*, *Grin1*, *Grin2a*, *Grin2b*, *Grm5*, *Itpr1*, *Plcb1*, *Plcb2*, *Plcb3*, *Ppp1r1a*, *Ppp3ca*, *Prkcb*
GABA receptor signaling	$2.65e^{-03}$	*Gabrg3*, *Kcnn3*, *Gad2*, *Kcnq2*, *Gabra4*, *Adcy5*, *Gabra6*, *Gabrb1*, *Gabra1*, *Gabra2*, *Gabrb2*
Calcium signaling	$3.42e^{-03}$	*Atp2a2*, *Atp2b1*, *Atp2b2*, *Camk2a*, *Camk2b*, *Camk4*, *Grin1*, *Grin2a*, *Grin2b*, *Hdac2*, *Itpr1*, *Myh7*, *Ppp3ca*, *Rcan1*, *Ryr1*, *Ryr3*
Protein kinase A signaling	$3.77e^{-03}$	*Adcy5*, *Camk2a*, *Camk2b*, *Camk4*, *Dusp5*, *Gnb5*, *Gng7*, *Itpr1*, *Nfkb1*, *Pde10a*, *Pde1b*, *Plcb1*, *Plcb2*, *Plcb3*, *Ppp1r1b*, *Ppp3ca*, *Prkcb*, *Ptk2b*, *Ptpn3*, *Ptpn5*, *Ryr1*, *Ryr3*, *Ywhaz*

including psychosis and depression, clinical symptoms frequently encountered in HD, and for other neurodegenerative diseases or psychiatric disorders. Accordingly, among 287 potential RARβ targets associated with HD, 40 genes are also related to pathophysiology of schizophrenia (Supplementary Table S1).

In addition to IPA- and DAVID-/GREAT-driven data mining, we compared our mouse ChIP-seq data with transcriptomic changes reported in caudate nucleus of HD patients [20]. Using this approach, we found that 678 genes containing RARβ binding sites displayed abnormal expression in human HD caudate samples (Supplementary Table S3), corresponding to 15 % of all transcripts found to be differentially expressed in the striatum of HD patients and such overlap was statistically significant ($p = 3.135e^{-5}$) as revealed using hypergeometric distribution analyses. Although this comparison does not take into account interspecies conservation of binding sites, such a high overlap supports the idea of a role of abnormal RARβ signaling in pathophysiology of HD.

Loss of RARβ Function Leads to HD-Like Transcriptional Changes and Indicates Direct Targets of RARβ in Mouse Striatum

Transcriptome Alterations in RARβ$^{-/-}$ NAcSh

The identification of RARβ binding sites by ChIP-seq analysis pointed to a large pool of genes which transcription may be controlled by RARβ. However, as suggested by previous studies [22, 26, 27], only a fraction of RAREs may be functional in physiological conditions, whereas the activity of others may become evident in pathological, pharmacological, or yet other specific conditions. Analysis of transcriptional changes in mice carrying a null mutation of RARβ provides a useful means to indicate functional binding sites, and to provide stronger candidates for RARβ targets. We performed such transcriptomic analysis on the ventral striatum (NAcSh), the region affected in HD [28, 29],

and the dysfunction of which may contribute to the three main aspects of HD pathophysiology, i.e., motor, cognitive, and affective abnormalities. Using Affymetrix GeneChip Mouse Gene 1.0 ST arrays, we identified 442 up-regulated and 614 down-regulated transcripts in the NAcSh of RARβ$^{-/-}$ mice (Fig. 2a, b). Such changes were significant as confirmed by Gene Set Enrichment Analysis (GSEA) analyses. IPA and DAVID analyses revealed that primary molecular and cellular functions affected by ablation of RARβ include cellular communication and development, carbohydrate metabolism, molecular transport, and small molecule biochemistry (Supplementary Table S4). Significant expression changes of a number of neurotransmitter receptors (e.g., *Cnr1*, *Chrm4*, *Drd3*, *Htr1b*), transporters (e.g., *Slc17a7*, *Slc17a8*, *Slc5a7*, *Slc20a1*), or metabolic enzymes (*Pde10a*, *Pde11a*, *Pde4b*) point to affected neurotransmission, synaptic signaling, metal ion transport, and metabolism of cyclic nucleotides. We also noted a deregulation of several genes encoding proteins involved in the control of calcium ion binding and signaling (e.g., *Calb1* and *2*, *Cacna2d3*, *Cadherins*, *Actn2*, *Kcnip1*). Analyses of signaling pathways revealed that the most significantly affected pathways are linked to G-protein signaling (cAMP-mediated signaling, $G_{\alpha i}$, and GPCR signaling, which were among the top 3 canonical pathways affected by ablation of RARβ; Supplementary Table S5). Such transcriptional changes are relevant to neurological and psychiatric conditions, including schizophrenia ($p = 2.57e^{-11}$), HD ($p = 3.19e^{-8}$), and mood disorders ($p = 3.89e^{-8}$). Specifically, 58 transcripts altered in the RARβ$^{-/-}$ NAcSh were reported by IPA analysis to be associated with HD pathophysiology (Table 2). The main functions affected by those alterations comprise calcium homeostasis, neurotransmission, G-protein signaling, and transcription. We compared our data with available transcriptomic data from caudate nucleus of HD patients [20]. Strikingly, 155 transcripts which expression was significantly affected (*t* test, $p \leq 0.05$) in RARβ$^{-/-}$ NAcSh were also altered in HD ($p = 0.037$, revealed using the hypergeometric distribution), which corresponds to 15 % of transcriptional changes in the murine RARβ$^{-/-}$ striatum and 3.5 % of all transcriptional changes in the striatum of HD patients (Supplementary Table S6).

Transcriptional Targets of RARβ in the Mouse Striatum

To further assess relevant RARβ targets, we compared our transcriptome data with genes assigned by ChIP-seq to contain at least one RARβ binding site. Among a total of 248 such genes, 103 were up-regulated and 145 were down-regulated (Fig. 2b; Supplementary Table S7). As expected, several genes known as direct transcriptional targets of RA were enriched in this group, including *Stra6*, *Dhrs3*, and *Chrm4*, but there were many genes not known so far for being RA-regulated. In order to gain insight into the functional consequences of ablation of RARβ, we performed functional annotation of those genes. IPA and DAVID annotations indicated that neurotransmission and cellular morphology (including microtubule dynamics, organization of cytoskeleton, and neuritogenesis) were among the primary cell functions associated with RARβ transcriptional target genes (Table 3). Although regulation of GPCR signaling by RARs was previously reported on evidence of transcriptional control of *Drd2* or *Oprk1* [13, 30], we have now extended the list of RARβ transcriptional targets to other GPCRs (e.g., *Chrm4*, *Gabrg3*, *Gpr88*), and other specific components of G-protein signaling pathways like *Rasd2*, *Rgs9*, *Pde10a*, and *Kcnk2*. We found significant deregulation of modulators of calcium homeostasis, including down-regulation of transcripts encoding ion channels (*Kcnip1*, *Cacna2d3*), and abnormal expression of genes which products indirectly control intracellular Ca^{2+} signaling (*Actn2*, *Strn*, *Nrgn*, *Scn4b*) (Supplementary Table S7).

In order to validate our transcriptomic data by qPCR, we chose 14 randomly selected genes associated with HD (Table 3), adding to this analysis *Rxrγ* and *Drd2*. These latter genes are known to be RA transcriptional targets which escaped our selection criteria for determination of RARβ binding sites in ChIP-seq (*Rxrγ*, BS at −25.4 kbp) and transcriptome fold change (*Drd2*, FC 0.81, $p = 4.9e^{-5}$). With exception of *Cnr1*, we confirmed all transcriptional changes which were detected by microarray analysis in the NAcSh (Fig. 2c). The most prominent down-regulations were observed for *Scn4b*, *Gpr88*, *Actn2*, *Tac1*, *Rasd2*, *Rgs9*, *Pde10a*, *Kcnk2*, *Cacna2d3*, *Gabrg3*, *Rxrγ*, *Drd2*, and *Kcnip1*, and up-regulation of *Nrgn* and *Synpr* was confirmed in the RARβ$^{-/-}$ NAcSh (Fig. 2c). Such changes were consistent with those observed in the striatum from human HD patients or R6/2 mice [20, 21, 31], with the exception of increased *Nrgn* and *Synpr* expression, and unchanged levels of *Cnr1* in RARβ$^{-/-}$ mice. Surprisingly, only few transcripts were also affected in the dorsal striatum (caudate putamen; CPu) of RARβ$^{-/-}$ mice (Fig. 2d). Indeed, only *Gabrg3*, *Nrgn*, and *Synpr* displayed similar magnitude of changes in CPu and in NAcSh, whereas *Scn4b* and *Tac1* displayed 2-fold weaker changes in the CPu, and *Cnr1* displayed an increased expression in the CPu, but not the NAcSh of RARβ$^{-/-}$ mice (compare Fig. 2c and d). Such differences suggest that RARβ signaling may be more sustained in the ventral striatum possibly due to higher availability of RA suggested by stronger expression of proteins involved in retinol transport and metabolism for example RBP1 (also known as CRBP1; [32]) and STRA6 [33].

RARβ Is Sequestered in Huntingtin Protein Aggregates in R6/2 Mouse Striatum

The strong reduction of RARβ transcripts observed in post-mortem caudate nucleus samples from HD patients [20] led to the hypothesis that reduced expression of this receptor and compromised RA signaling could contribute to the pathophysiology of HD. Whereas our analyses of RARβ transcriptional

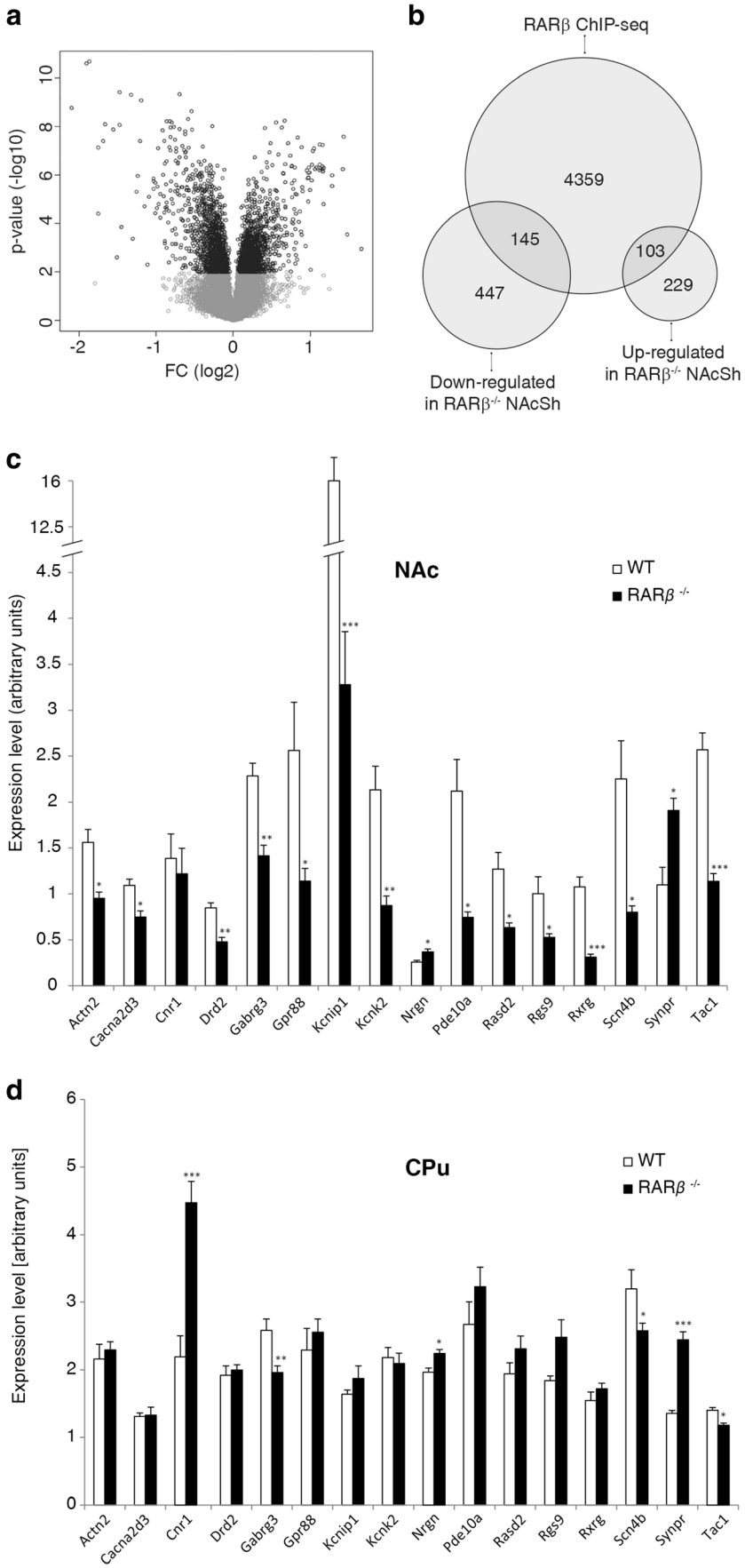
a
p-value (-log10)
FC (log2)
b
RARβ ChIP-seq
4359
145
103
229
447
Up-regulated in RARβ-/- NAcSh
Down-regulated in RARβ-/- NAcSh
c
NAc
WT
RARβ -/-
Expression level (arbitrary units)
Actn2
Cacna2d3
Cnr1
Drd2
Gabrg3
Gpr88
Kcnip1
Kcnk2
Nrgn
Pde10a
Rasd2
Rgs9
Rxrg
Scn4b
Synpr
Tac1
d
CPu
WT
RARβ -/-
Expression level [arbitrary units]

◀ **Fig. 2** Transcriptional targets of RARβ. **a** Volcano plot representing transcriptional changes in the NAcSh of RARβ$^{-/-}$ mice. The fold changes (*FC*) of gene expression in RARβ$^{-/-}$ NAcSh were calculated with respect to WT NAcSh, and are illustrated on the horizontal axis using a logarithmic scale. *Vertical axis* represents the corresponding *p* values. The significance cutoff was set at $p = 0.01$, which corresponds to a false discovery rate (FDR) of 0.09. **b** Venn diagram representing the overlap between genes assigned with RARβ binding regions as determined by ChIP-seq, and genes altered in expression in the NAcSh of RARβ$^{-/-}$ mice, as determined by transcriptomics. **c**, **d** qPCR analysis of transcriptional targets of RARβ in the NAcSh and CPu, respectively. The genes selected for analysis correspond to transcripts with impaired expression in Huntington's disease.*$p < 0.05$; **$p < 0.01$; ***$p < 0.001$

target genes support and elaborate this hypothesis, it is not clear whether and how reduction of RARβ receptor level is attained in HD. To address these points, we analyzed RARβ expression and its subcellular distribution in ventral and dorsal regions of the striatum of R6/2 transgenic mice, a widely employed model of Huntington's disease [34]. Real-time quantitative PCR revealed a significant reduction of RARβ mRNA in early symptomatic R6/2 mice, in the NAcSh (2.85 ± 0.43 arbitrary units for wild-type (WT) and 1.32 ± 0.18 for R6/2, *t* test, $p = 0.0004$) and CPu (2.27 ± 0.22 arbitrary units for WT and 0.98 ± 0.18 for R6/2, *t* test, $p = 0.002$). RARβ expression was not affected prior to aggregate formation in the developing striatum of R6/2 mice at E18.5 (0.256 ± 0.02 arbitrary units for WT and 0.222 ± 0.06 for R6/2; ns). Using immunofluorescent detection, we observed abundant expression of RARβ in the CPu and NAcSh of adult WT mice, but this expression was decreased in R6/2 mice (Fig. 3a, b) and absent in RARβ$^{-/-}$ mice (Supplementary Fig. S1). Quantitative immunofluorescence analyses using the Imaris software revealed that the amount of RARβ protein was significantly (on average ~50 %) reduced in R6/2 mice in both CPu (*t* test, $p = 2.36e^{-5}$) and NAcSh (*t* test, $p = 3.46e^{-6}$), as illustrated by lower numbers of cells displaying strong expression of RARβ (Fig. 3c). To address the mechanism of such reduction, we investigated whether low RARβ expression may result from its sequestration within HTT aggregates in R6/2 mice. Analyses of RARβ distribution within the nuclei of individual cells in R6/2 striatum revealed about 1.75-times higher levels of RARβ signal in HTT aggregates, as compared to the other regions of the nuclei, and such enrichment was observed in both the CPu (*t* test, $p = 3.4e^{-19}$) and NAcSh (*t* test, $p = 8.1e^{-18}$) (Fig. 3b, d). That such a colocalization reflects partial sequestration of RARβ in HTT aggregates is also supported by absence of RARβ foci in R6/2 transgenic striatum prior to aggregate formation during prenatal stage of brain development (Supplementary Fig. S2). We also observed a significant reduction of cell density in the NAcSh (3253 ± 343 cells/mm^2 for WT and 1998 ± 166 for R6/2), but not in the CPu (1743 ± 177 cells/mm^2 for WT and 2225 ± 207 for R6/2), of R6/2 transgenic mice. Such region-selective cell decrease was supported by significant interaction between the *genotype* and *striatal sub-region* for cell counts in two-way ANOVA analyses ($F_{[1, 32]} = 12.8$; $p = 0.001$).

Structural Analysis of RARβ Binding Sites

Our study provides the first in vivo data on RAR binding sites in the brain. We analyzed the genomic architecture of these binding sites. Using the Homer software [35], we found that binding sites were highly enriched in core promoters (±50 bp from the TSS) and proximal promoter regions (−300 to −50 bp), where they appeared 10 times more frequent than in distal promoter regions (−5000 to −300 bp) or gene body (+50 bp to transcription termination site) (Fig. 4a). However, whereas binding sites located within the promoter (core, proximal and distal) represented 24 % of all regions occupied by RARβ, the majority (55 %) of binding sites were mapped to the gene body and 21 % to intergenic locations (Fig. 4b). The distribution of RARβ binding sites in the promoter regions was similar to DNA occupation by H3K4me3 (Fig. 4c). SeqMINER clustering analyses of RARβ and H3K4me3 binding sites with respect to their distribution profiles and TSS proximity revealed that for the total of 6273 Ensembl transcripts (Homer genomic annotation), 3640 were located within ±5 kbp from the TSS and colocalized with H3K4me3 binding regions (Fig. 4d). For 1045 of those transcripts, RARβ and H3K4me3 occupied large DNA regions extending from the TSS towards gene body (cluster 1, Fig. 4d). More frequently (2595 transcripts), such an overlap was restricted to a narrow region localized in the vicinity of the TSS (cluster 2, Fig. 4d), whereas for 2633 transcripts there was no overlap between RARβ and H3K4me3 binding sites within ±5 kbp (cluster 3, Fig. 4d).

Globally, the binding sites were composed of different forms of repeated sequences previously described as binding sites for RA receptors [36–38], and characterized by the presence of two consensus half-sites (RGKTCA) with variable spacing and orientation. Our ChIP-seq analysis revealed that RARβ occupies a large repertoire of direct repeats (DR0–DR10), inverted repeats (IR0–IR10), and everted repeats (ER0–ER10) (Fig. 5). These three types of elements were previously reported from ChIP-seq analyses in murine embryonic stem cells and embryonal carcinoma F9 cells using a pan-RAR (recognizing all three RARs) antibody [39]. As expected, DRs were the most frequently encountered RAREs, representing 79 % out of 957 consensus binding elements (no mismatch from consensus) (Fig. 5a). Among 957 elements, DR0 were the most represented (188), followed closely by DR2 (174) and DR5 (172) (Fig. 5b). We also identified about 130 highly conserved IRs and a similar number of ERs, with IR0, ER8, and ER10 as the most frequently encountered (Fig. 5c, d). Often several different elements were present within a single peak corresponding to a RARβ occupied DNA region. As determined with the help of regulatory

Table 2 Transcripts associated with HD pathophysiology and quantitatively affected in the NAcSh of RARβ$^{-/-}$ mice

Gene symbol	Gene name	Fold change RARβ$^{-/-}$/WT	Location	Type
Actn2	Actinin, alpha 2	0.78	Nucleus	Transcription reg.
Ankrd2	Ankyrin repeat domain 2 (stretch responsive muscle)	1.21	Nucleus	Transcription reg.
Ascl1	Achaete-scute family bHLH transcription factor 1	1.23	Nucleus	Transcription reg.
Bhlhe40	Basic helix-loop-helix family, member e40	1.25	Nucleus	Transcription reg.
C4b	Complement component 4B (Childo blood group)	1.29	Extracellular space/plasma membrane	Other
Cacna2d3	Calcium channel, voltage-dependent, alpha 2/delta subunit 3	0.78	Plasma membrane	Ion channel
Calb1	Calbindin 1, 28 kDa	1.94	Cytoplasm	Other
Casq2	Calsequestrin 2 (cardiac muscle)	1.73	Cytoplasm	Other
Cd38	CD38 molecule	0.67	Plasma membrane	Enzyme
Chrm4	Cholinergic receptor, muscarinic 4	0.79	Plasma membrane	GPCR
Chrm5	Cholinergic receptor, muscarinic 5	1.75	Plasma membrane	GPCR
Cnr1	Cannabinoid receptor 1 (brain)	1.26	Plasma membrane	GPCR
Ctgf	Connective tissue growth factor	1.76	Extracellular space	Growth factor
Dhcr7	7-Dehydrocholesterol reductase	0.78	Cytoplasm	Enzyme
Drd3	Dopamine receptor D3	0.66	Plasma membrane	GPCR
Dynlt1	Dynein, light chain, Tctex-type 1	0.72	Cytoplasm	Other
Flrt2	Fibronectin leucine rich transmembrane protein 2	0.71	Plasma membrane	Other
Gabra5	Gamma-aminobutyric acid (GABA) A receptor, alpha 5	1.39	Plasma membrane	Ion channel
Gabrg3	Gamma-aminobutyric acid (GABA) A receptor, gamma 3	0.78	Plasma membrane	Ion channel
Gfap	Glial fibrillary acidic protein	1.25	Cytoplasm	Other
Gpr88	G protein-coupled receptor 88	0.77	Plasma membrane	GPCR
Grin3a	Glutamate receptor, ionotropic, n-methyl-D-aspartate 3A	1.29	Plasma membrane	Ion channel
Hmgcs2	3-Hydroxy-3-methylglutaryl-coA synthase 2 (mitochondrial)	1.25	Cytoplasm	Enzyme
Hspa1a	Heat shock protein 1A	1.27	Other	Other
Hspa8	Heat shock 70 kDa protein 8	0.56	Cytoplasm	Enzyme
Htr1b	5-Hydroxytryptamine (serotonin) receptor 1B, G protein-coupled	1.25	plasma membrane	GPCR
Id4	Inhibitor of DNA binding 4, dominant negative helix-loop-helix protein	1.33	Nucleus	Transcription reg.
Ivns1abp	Influenza virus nS1A binding protein	0.64	Nucleus	Other
Kcnip1	Kv channel interacting protein 1	0.36	Plasma membrane	Ion channel
Kcnk2	Potassium channel, subfamily K, member 2	0.59	Plasma membrane	Ion channel
Man1a1	Mannosidase, alpha, class 1A, member 1	1.33	Cytoplasm	Enzyme
Nefl	Neurofilament, light polypeptide	0.62	Cytoplasm	Other
Npy	Neuropeptide Y	1.31	Extracellular space	Other
Nrgn	Neurogranin	1.35	Plasma membrane	Other
Oprk1	Opioid receptor, kappa 1	0.36	Plasma membrane	GPCR
Pde10a	Phosphodiesterase 10A	0.73	Cytoplasm	Enzyme
Plscr4	Phospholipid scramblase 4	1.28	Plasma membrane	Enzyme

Table 2 (continued)

Gene symbol	Gene name	Fold change RARβ$^{-/-}$/WT	Location	Type
Ppargc1a	Peroxisome proliferator-activated receptor gamma, coactivator 1 alpha	0.74	Nucleus	Transcription reg.
Rarb	Retinoic acid receptor, beta	0.27	Nucleus	Ligand-depend. nuclear receptor
Rasd2	RASD family, member 2	0.73	Cytoplasm	Enzyme
Rbp4	Retinol binding protein 4, plasma	1.41	Extracellular space	Transporter
Rgs14	Regulator of G-protein signaling 14	1.29	Cytoplasm	Other
Rgs9	Regulator of G-protein signaling 9	0.75	Cytoplasm	Enzyme
Rhobtb3	Rho-related BTB domain containing 3	0.78	Cytoplasm	Enzyme
Rxrg	Retinoid X receptor, gamma	0.53	Nucleus	Ligand depend. nuclear receptor
Scn4b	Sodium channel, voltage-gated, type IV, beta subunit	0.51	Plasma membrane	Ion channel
Serpini1	Serpin peptidase inhibitor, clade I (neuroserpin), member 1	1.26	Extracellular space	Other
Sgk1	Serum/glucocorticoid regulated kinase 1	1.25	Cytoplasm	Kinase
Sh3bp4	SH3-domain binding protein 4	1.31	Cytoplasm	Other
Slc17a7	Solute carrier family 17 (vesicular glutamate transporter), member 7	1.88	Plasma membrane	Transporter
Slc35d3	Solute carrier family 35, member D3	0.64	Other	Other
Slit2	Slit homolog 2 (Drosophila)	0.71	Extracellular space	Other
Slmap	Sarcolemma associated protein	0.76	Plasma membrane	Other
Synpr	Synaptoporin	1.34	Plasma membrane	Transporter
Tac1	Tachykinin, precursor 1	0.75	Extracellular space	Other
Tbr1	T-box, brain, 1	1.95	Nucleus	Transcription reg.
Vcan	Versican	0.76	Extracellular space	Other
Zbtb16	Zinc finger and BTB domain containing 16	1.33	Nucleus	Transcription reg.

sequence analysis tools (RSAT) [40], 257 peaks also harbored consensus binding sites for estrogen-related receptors α and β (ESRRA and ESRRB).

Among 248 RARβ transcriptional targets (bearing RARβ-binding sites and which expression was altered in RARβ$^{-/-}$ mice), only 64 (25 %) contained conserved DRs, IRs, and ERs. Since the population of highly conserved RAREs was poorly represented in this group of genes, we performed additional search for RAREs, allowing one mismatch in the RARE half-site consensus sequence. This led to the detection of a total of 833 motifs, which were attributed to 174 out of 248 genes (70 %). Despite an overall increase of RARE-like elements, suggesting a high flexibility of RARβ in DNA recognition, the distribution between different RARE subtypes was not remarkably affected, with the number of DRs decreased only from 70 to 60 % in favor of an increase of IRs and ERs (20 % each). When searching the pool of 248 genes for RAREs with consensus half-sites or allowing one mismatch, DR5, DR0, DR7, and DR2 were most represented motifs. A de novo motif search in RARβ-occupied loci that did not contain RAREs revealed the presence of one or more Sp1-binding motifs within 50 % of such RARβ-bound regions.

To gain insight into the mechanisms of RARβ-dependent transcriptional control, we searched for core promoter elements (CPE; for review see [41]) in the core promoter region (±50 bp from the TSS) of the 248 RARβ transcriptional targets. Surprisingly, when searching for eight known CPE consensus sequences (TATA box, BRE^{u}, BRE^{d}, Inr, DPE, DCE, MTE, or XCPE1), we did not find any TATA box, but mostly detected Inr (18 %), DPE (13 %), BRE^{d} (12 %), and BRE^{u} (7 %). Focusing these analyses on 29 genes associated with

Table 3 Neurological diseases and functional annotations associated with 248 potential striatal direct targets of RARβ

Disease/functional annotation	*p* value	Nb	Gene symbols
Huntington's disease	$2.26e^{-08}$	29	*Actn2*, *Cacna2d3*, *Chrm4*, *Cnr1*, *Dynlt1*, *Flrt2*, *Gabrg3*, *Gpr88*, *Hspa*, *Htr1b*, *Ivns1abp*, *Kcnip1*, *Kcnk2*, *Man1a1*, *Nrgn*, *Pde10a*, *Rarb*, *Rasd2*, *Rgs9*, *Scn4b*, *Sgk1*, *Sh3bp4*, *Slc35d3*, *Slmap*, *Synpr*, *Tac1*, *Vcan*, *Zbtb*, *Znf385b*
Neuromuscular disease	$3.84e^{-06}$	32	*Actn2*, *Adora1*, *Cacna2d3*, *Chrm4*, *Cnr1*, *Dynlt1*, *Fhit*, *Flrt2*, *Gabrg3*, *Gpr88*, *Hspa8*, *Htr1b*, *Ivns1abp*, *Kcnip1*, *Kcnk2*, *Man1a1*, *Nrgn*, *Pde10a*, *Pde4b*, *Rarb*, *Rasd2*, *Rgs9*, *Scn4b*, *Sgk1*, *Sh3bp4*, *Slc35d3*, *Slmap*, *Synpr*, *Tac1*, *Vcan*, *Zbtb16*, *Znf385b*
Mood disorders	$9.70e^{-06}$	20	*Cdc25b*, *Chrm4*, *Dach1*, *Esr1*, *Gabrg3*, *Htr1b*, *Kcnh2*, *Kcnk2*, *Mchr1*, *Mical2*, *Pde10a*, *Pde11a*, *Reln*, *Scn4b*, *Sgk1*, *Spry2*, *Tac1*, *Thrb*, *Tle4*, *Wfs1*
Neurotransmission	$1.07e^{-05}$	18	*Adora1*, *Cdh8*, *Chrm4*, *Cnr1*, *Dlgap1*, *Epb41*, *Fstl1*, *Grm8*, *Htr1b*, *Kcnh2*, *Kcnip1*, *Nefm*, *Nrgn*, *Rarb*, *Rasd2*, *Reln*, *Tnr*, *Unc13a*
Cognition	$3.81e^{-05}$	17	*Adora1*, *Chl1*, *Cnr1*, *Epb41*, *Esr1*, *Htr1b*, *Mchr1*, *Mme*, *Npas2*, *Nxph3*, *Pde11a*, *Rarb*, *Sgk1*, *Stra6*, *Tac1*, *Thrb*, *Tnr*
Neuritogenesis	$6.59e^{-05}$	18	*Chl1*, *Cnr1*, *Dynlt1*, *Enc1*, *Gda*, *Nefm*, *Ntng1*, *Pard3*, *Prkg1*, *Ptprm*, *Reln*, *Robo2*, *Scn4b*, *Sema3a*, *Sgk1*, *Slit3*, *Strn*, *Tpbg*
Movement disorders	$1.11e^{-04}$	33	*Actn2*, *Adora1*, *Cacna2d3*, *Chrm4*, *Cnr1*, *Dynlt1*, *Flrt2*, *Gabrg3*, *Gpr88*, *Hspa8*, *Htr1b*, *Ivns1abp*, *Kcnh2*, *Kcnip1*, *Kcnk2*, *Man1a1*, *Nrgn*, *Pde10a*, *Pde4b*, *Rarb*, *Rasd2*, *Reln*, *Rgs9*, *Scn4b*, *Sgk1*, *Sh3bp4*, *Slc35d3*, *Slmap*, *Synpr*, *Tac1*, *Vcan*, *Zbtb16*, *Znf385b*
Bipolar disorder	$1.17e^{-04}$	14	*Cdc25b*, *Chrm4*, *Dach1*, *Esr1*, *Gabrg3*, *Htr1b*, *Kcnh2*, *Mchr1*, *Reln*, *Scn4b*, *Spry2*, *Thrb*, *Tle4*, *Wfs1*
Depressive disorder	$2.12e^{-04}$	12	*Chrm4*, *Esr1*, *Gabrg3*, *Kcnh2*, *Kcnk2*, *Mical2*, *Pde10a*, *Pde11a*, *Sgk1*, *Tac1*, *Thrb*, *Wfs1*
Psychosis	$8.32e^{-04}$	6	*Chrm4*, *Esr1*, *Gabrg3*, *Htr1b*, *Kcnh2*, *Tac1*
Loss of neurons	$1.35e^{-03}$	7	*Fig4*, *Lmx1b*, *Mfge8*, *Mme*, *Tac1*, *Tgfa*, *Thrb*
Locomotion	$1.38e^{-03}$	12	*Chl1*, *Cnr1*, *Esr1*, *Fig4*, *Htr1b*, *Npas2*, *Pde10a*, *Pde11a*, *Rarb*, *Rasd2*, *Reln*, *Strn*
Anxiety	$1.77e^{-03}$	8	*Adora1*, *Chl1*, *Cnr1*, *Grm8*, *Htr1b*, *Mchr1*, *Rasd2*, *Tac1*
Anxiety disorders	$1.83e^{-03}$	6	*Cacna2d3*, *Cnr1*, *Esr1*, *Gabrg3*, *Htr1b*, *Tac1*
Tauopathy	$2.60e^{-03}$	17	*Chl1*, *Chrm4*, *Cnr1*, *Esr1*, *Gabrg3*, *Gc*, *Grm8*, *Htr1b*, *Larp4*, *Lphn2*, *Mfge8*, *Mme*, *Nrgn*, *Pcdh11x/Pcdh11y*, *Reln*, *Scarb1*, *Scn4b*
Activation of neurons	$3.59e^{-03}$	4	*Cnr1*, *Gja5*, *Pde11a*, *Tac1*
Dendritic growth/branching	$3.75e^{-03}$	7	*Cnr1*, *Gda*, *Nefm*, *Reln*, *Robo2*, *Scn4b*, *Tpbg*
Development of brain	$4.58e^{-03}$	14	*Chl1*, *Cnr1*, *Dscaml1*, *Ext1*, *Lmx1b*, *Myo16*, *Pard3*, *Prkg1*, *Rarb*, *Reln*, *Robo2*, *Slit3*, *Spry2*, *Thrb*
Abnormal morphology of neurons	$6.55e^{-03}$	12	*Chl1*, *Cntn6*, *Lmx1b*, *Nefm*, *Ptpn13*, *Robo2*, *Sema3a*, *Spry2*, *Thrb*, *Tnr*, *Unc13a*, *Vcan*
Action potential of nervous tissue	$7.12e^{-03}$	4	*Adora1*, *Cnr1*, *Rarb*, *Thrb*
Alzheimer's disease	$8.79e^{-03}$	15	*Chl1*, *Chrm4*, *Cnr1*, *Esr1*, *Gabrg3*, *Gc*, *Grm8*, *Larp4*, *Lphn2*, *Mfge8*, *Mme*, *Nrgn*, *Pcdh11x/Pcdh11y*, *Reln*, *Scarb1*
Major depression	$1.08e^{-02}$	7	*Gabrg3*, *Kcnk2*, *Mical2*, *Pde10a*, *Pde11a*, *Sgk1*, *Wfs1*

HD, we did not find enrichment of any specific CPE. However, we noticed that 25 out of these 29 genes belonged to cluster 1, which is characterized by a broad occupation pattern of H3K4me3 (Fig. 4d), in contrast with the full set of 248 genes which were distributed approximately equally across the three clusters.

Discussion

Retinoic acid is indispensable for normal development of many organs including the brain, but its role in the adult central nervous system (CNS) is poorly recognized. One of the central reasons could be that availability of RA is highly

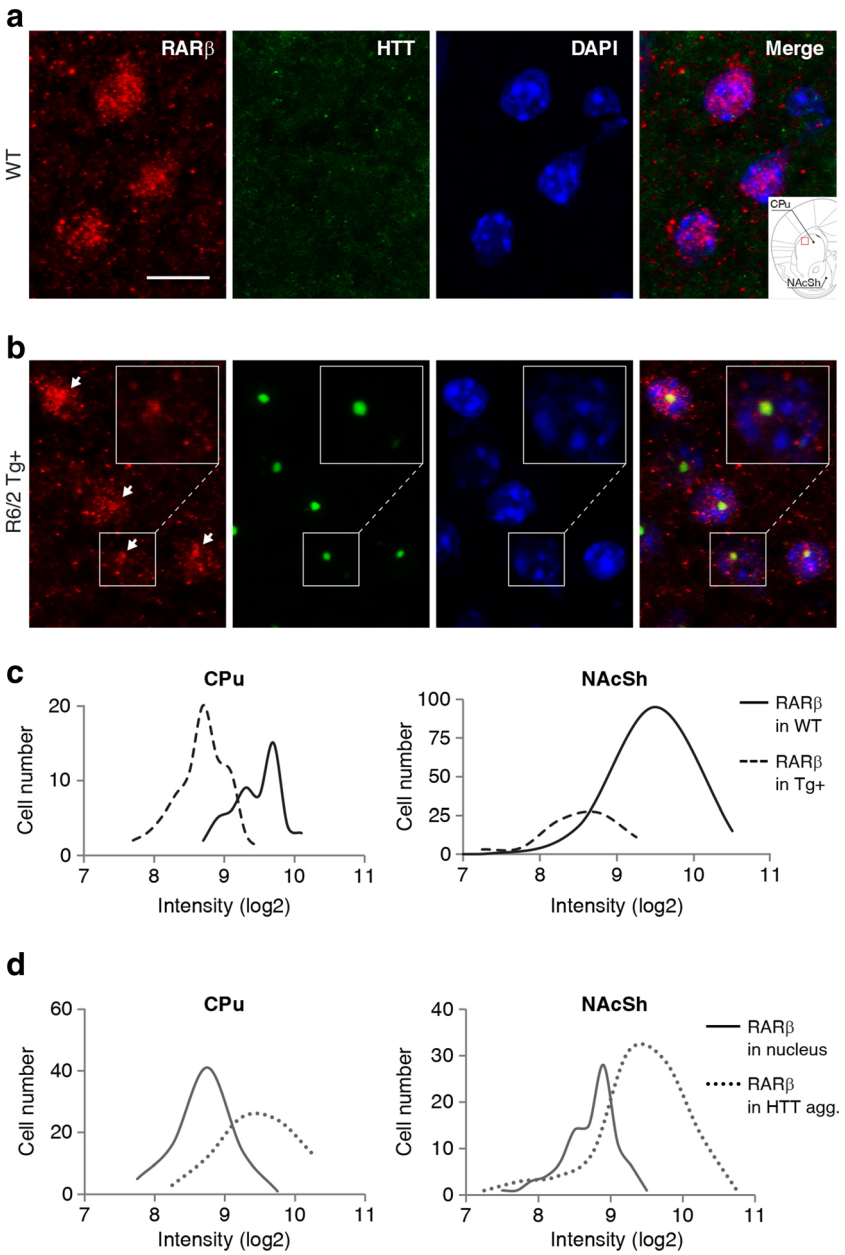

Fig. 3 Quantitative analyses of RARβ expression in the striatum of R6/2 mice. **a**, **b** Immunofluorescence detection of RARβ (*red*) and HTT (*green*) in coronal sections of the CPu in 9-week-old WT (*upper panels*) and R6/2 transgenic mice (*lower panels*). The region displayed is boxed in the scheme inserted in *lower corner* of **a**. The magnification of RARb and HTT colocalization was shown in the plane of HTT aggregate in the *upper right corner* of the **b**. DAPI-stained nuclei are shown in *blue*. *Scale bar*, 10 μm. **c** Quantitative analysis of RARβ expression is shown as number of cells displaying different intensities of RARβ signal in CPu and NAcSh of WT and R6/2 mice. **d** Intensity of RARβ labeling detected by immunofluorescence within HTT aggregates is compared to its levels in other regions of the nucleus, in CPu and NAcSh of R6/2 mice. *CPu*, caudate putamen; *NAcSh*, nucleus accumbens shell

secured in the brain by homeostatic mechanisms involving its local synthesis and/or peripheral metabolism. Thus, manifestations of abnormal control of brain functions by the RA pathway may become apparent only in cases of extreme vitamin A deficiency or in pathological conditions. To uncover such functions, it is critical to identify molecular substrates of RA signaling, including direct transcriptional targets of its receptors.

RARβ Regulated Signaling Pathways and Cell Functions

Using chromatin immunoprecipitation followed by high throughput sequencing (ChIP-seq), we have identified genomic RARβ binding sites in the mouse striatum, the main domain of RARβ expression in the brain [2], and the key brain region involved in control of a number of psychomotor functions [14]. Among 4607 genes bearing at least one binding site, we identified 248 which transcription was altered in the striatum of RARβ$^{-/-}$ mice (as detected in our comparative transcriptomic analysis of the NAcSh of WT and RARβ$^{-/-}$ mice). Those genes are proposed as strong candidates for being direct transcriptional targets of RARβ. Their functional annotations point to GPCR signaling as one of the major pathways regulated by RARβ. In particular, we identified new transcriptional targets like *Drd3*, *Gpr88*, or cAMP catabolic enzymes (*Pde10a*, *Pde4b*, *Pde1b*), and we determined in vivo RARβ-binding sites for genes previously reported as being regulated by RA, for example *Stra6*, *Cnr1*, *Chrm4*, *Drd2*, or

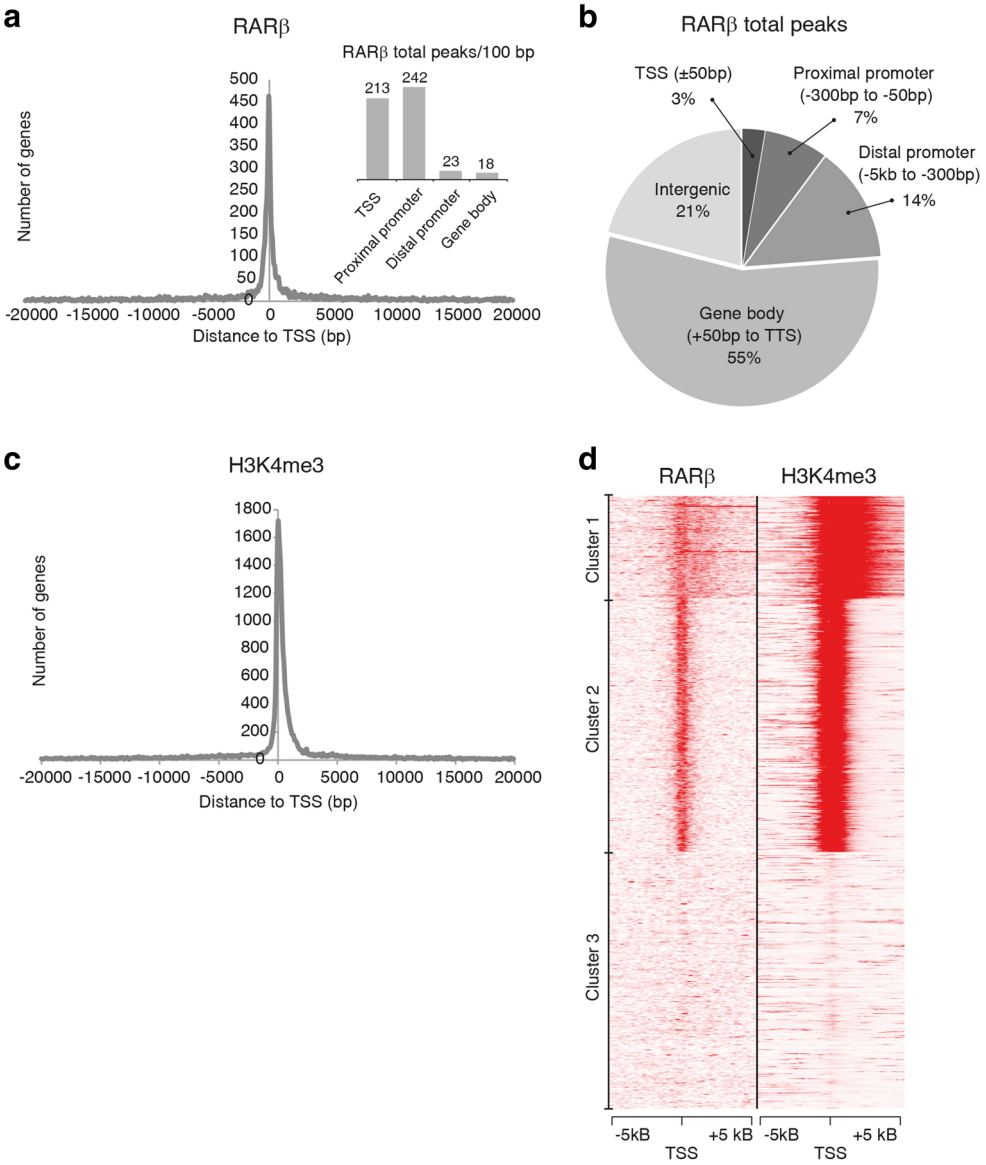

Fig. 4 Characterization of striatal profiles of RARβ and H3K4me3 DNA-binding sites. **a** Genomic position of RARβ binding sites with respect to transcription start sites (*TSS*). **b** Genomic annotation for RARβ binding sites. Distribution of RARβ binding regions within the genome was set-up using Homer. The following location criteria were used based on the distance from TSS: core promoter ±50 bp, proximal promoter −300 to −50 bp, distal promoter −5 kbp to −300 bp, gene body +50 bp to transcription termination site (*TTS*), intergenic (variable lengths). **c** Genomic position of H3K4me3 binding sites with respect to TSS. **d** Comparative clustering of RARβ and H3K4me3 ChIP-seq data using seqMINER. Read densities were established as regions surrounding the set of TSS of mouse genes based on Ensembl (v.67). Tag densities from each ChIP-seq data set were collected in a window of 10 kbp encompassing the TSS. The collected values were subjected to k-means clustering coupled to linear normalization. The intensity of H3K4me3 was lowered 10-fold

Nrgn [13, 39, 42, 43]. Analyzing the potential impact of such regulations on dopaminergic (DRD1- and DRD2-mediated) signaling can be particularly instructive about RARβ control of striatal functions, as cell type-specific expression of DRD1 and DRD2 identifies, respectively, striatonigral and striatopallidal GABAergic projection neurons, which constitute the two main striatal outputs pathways. Imbalanced signaling through these pathways has been suggested to underlie symptoms of several neuropsychiatric disorders including HD and PD, as well as drug addiction and depression (for review, see [14, 44]). RARβ may be required for the activity of both pathways, contributing at multiple levels to their balanced signaling. Our data indicate that RARβ deficiency may lead to compromised activities of DRD2-positive striatopallidal pathway, resulting from concomitant reduction of transcription of *Drd2* and *Pde10a*, the latter coding for a cAMP-catabolizing enzyme (phosphodiesterase) functionally associated with DRD2 activities [45].

Among direct transcriptional targets of RARβ, we also found the gene encoding cannabinoid receptor 1 (*Cnr1*), which displayed the most prominent increase of expression among genes that were tested by qPCR in the CPu of RARβ$^{-/-}$ mice. A consequence of enhanced *Cnr1* expression would be an inhibition of DRD1 and DRD2 signaling, as previously suggested [46], but such effect would be limited to the CPu as no significant increase of *Cnr1* expression was noted in the NAcSh of mutant mice. An inhibitory effect of CNR1 on adenylate cyclase activity may contribute to control of DA receptor signaling, but more importantly may lead to an overall reduction of cAMP availability in the RARβ$^{-/-}$ striatum. Although the net effect of opposing expression changes of *Cnr1* and *Pde10a*, *Pde1b*, and *Pde4b* on cAMP levels need

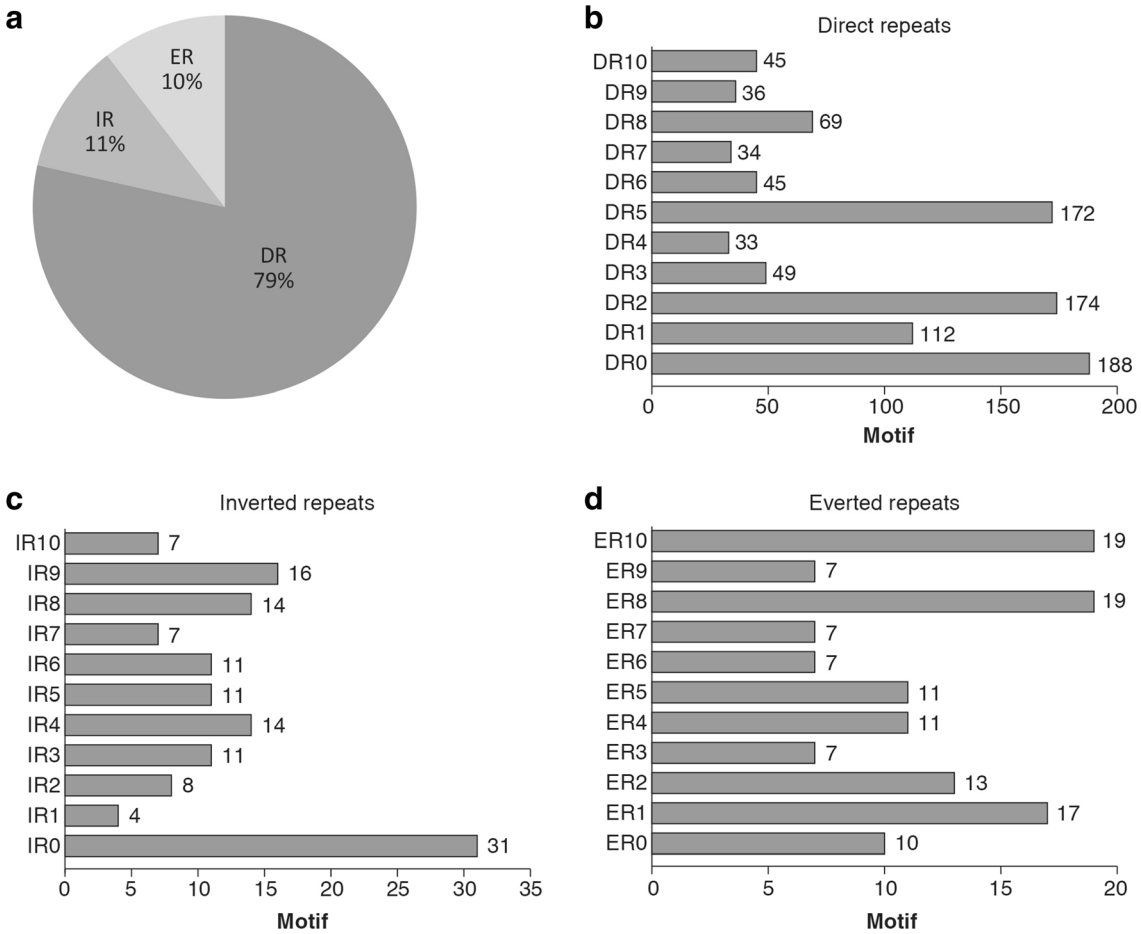

Fig. 5 Consensus RA-response elements (RAREs) in RARβ-bound loci. **a** Overview of the frequency of direct repeats (*DR*), inverted repeats (*IR*), and everted repeats (*ER*) of the consensus RARE half-site (RGKTCA) identified through our bioinformatics analysis of RARβ-bound loci. **b**–**d** Distribution of DRs (**b**), IRs (**c**), and ERs (**d**) according to the spacing between half-sites (numbers from 0 to 10 refer to the number of base pairs separating the half-sites)

to be addressed experimentally, we cannot exclude the possibility of cell type-specific changes in cAMP availability.

Functional annotations of direct transcriptional targets of RARβ also point to a multilevel control of calcium homeostasis and signaling, which in absence of RARβ may be impaired and possibly harmful to striatal neurons. Thus, reduced expression of *Cacna2d3*, the subunit of Ca^{2+} channel known to limit action potential-driven Ca^{2+} influx [47], may lead to increased intracellular Ca^{2+} levels following neuronal activation in RARβ$^{-/-}$ mice. Similarly, down-regulation of the Ca^{2+} sensor KCNIP1, a critical subunit of potassium Kv4 channel, may lead to prolonged neuronal depolarization periods during action potentials, which in turn would result in extended duration of activity-driven Ca^{2+} influx. In contrast, reduction of *Actn2* and *Rgs9* expression in RARβ$^{-/-}$ mice could act to counterbalance increased Ca^{2+} influx. Synaptic communication and plasticity could be further affected due to inefficient utilization and signaling of intracellular and synaptic Ca^{2+}, which is controlled by STRN and NRGN, both being direct targets of RARβ transcriptional activity [48, 49].

RARβ and Central Nervous System Disorders

Reduced RA signaling has been associated with several neurodegenerative diseases including AD, HD, or PD. Our analyses provide evidence for a strong association between RARβ loss of function and pathophysiology of HD, and suggest mechanisms through which compromised RA signaling may contribute to other neurodegenerative diseases including AD and PD. A link between RARβ and HD was suggested by previous transcriptomic studies of HD patients [20] or mouse models [21, 31]. Here, we report that expression of RARβ is significantly reduced at transcript and protein level in early symptomatic R6/2 mice, a transgenic mouse model of HD. We also show that such a reduction may result from partial sequestration of RARβ in aggregates of mutant HTT protein, which may further compromise RARβ signaling. The mechanism of sequestration is not known; thus, we cannot exclude direct interactions of RARβ with mutant HTT, and/or indirect co-sequestration of RARβ with CBP and N-CoR, which are known to interact both, with RARs [50, 51] and with mutant HTT [52, 53].

Our genome-wide identification of RARβ binding sites allowed to establish a list of potential RARβ transcriptional targets in the striatum, which is highly enriched in genes which expression is affected in HD patients. Functional annotation of 287 such genes pointed to the possibility of a RARβ-dependent multilevel control of mitochondrial functions, including oxidative phosphorylation. Although RARβ-dependent regulation of those genes remains to be formally demonstrated, deficient control of mitochondrial functions may provide a mechanistic link between pathophysiology of HD, or other neurodegenerative diseases for which compromised RA signaling has been documented [15–18, 21, 54], and which all show mitochondrial abnormalities (for review see [55]).

Among genes with RARβ binding sites, we also identified a number of transcriptional regulators which are specifically associated with HD, but not AD or PD. Such observation supports a hypothesis on the pathogenic mechanism of HD, which involves global deficits in activity of different transcription factors [56, 57]. One of such mechanisms is sequestration and reduced availability of several ubiquitous transcription factors like CBP, N-CoR, p53, Sp1, TAF4 (TAFII130), and TBP [52, 53, 58–62]. Reduced RARβ levels in HD could also indirectly impact transcription in the striatum by affecting expression of RNA polymerase II subunits (*Polr2a*, *Polr2i*), several transcription factors (e.g., *Meis2*, *Sp1*, *Notch2*, *Foxp1*, *Nr1d1*) and cofactors (e.g., *Ppargc1a*, *Rcor1*), and chromatin-modifying enzymes (e.g., *Hdac2*, *Kdm3a*), all of which except *Polr2a* and *Rcor1* are known to be impaired in HD [20, 63–65]. RARβ could also indirectly impact transcription by direct regulation of *Foxp1* expression, another transcription factor implicated in HD [66]: indeed, we found several indirect targets of RARβ known to be regulated by FOXP1 in striatal cells.

Further insight into RARβ effects on general transcription mechanisms comes from detailed analyses of RARβ binding sites in 29 genes which expression was affected in the RARβ$^{-/-}$ striatum as well as in HD. These analyses revealed that in HD-relevant transcriptional targets, the RARβ binding sites overlapped with broad peaks of H3K4me3 occupation, shown to ensure the precision and robustness of gene expression which should be particularly high in tissues where function of a given gene is critical [67]. Intriguingly, none of the HD-associated RARβ transcriptional targets contained a TATA box in their promoter, suggesting that transcriptional control by RARβ does not directly involve TBP, but possibly other TBP-associated factors (TAFs). It is tempting to speculate that TATA-less gene promoters could be particularly susceptible to compromised RARβ signaling, suggesting also that such promoters rarely used in studies of retinoid signaling may be in fact more suitable than TATA box-containing promoters for testing the functionality of RAREs.

A Dorso-ventral Gradient of Increasing Susceptibility to RARβ Signaling in the Striatum

Transcriptomic analysis of RARβ$^{-/-}$ mice revealed significant alterations in gene expression in the NAcSh, which were confirmed for a selected group of genes using qPCR. Strikingly, only few of such transcriptional changes were also observed in the CPu. Our data therefore indicate an important regional specificity in RA control of gene transcription, as there appears to be a clear dorso-ventral gradient of increasing transcriptional effects of RA signaling in the striatum. A high susceptibility of the NAcSh to altered RA signaling may be of relevance for understanding some aspects of cognitive and affective symptoms observed in neurodegenerative disorders associated with reduced RA signaling. In particular, compromised GPCRs signaling may underlie depressive-like symptoms in the context of neurodegeneration, and may contribute to the pathophysiology of some psychiatric diseases such as depression or schizophrenia [5, 68–70]. RARβ-controlled signaling pathways revealed in our study indicate that reduced RA signaling may contribute to the atrophy of NAcSh, one of the important symptoms of HD, PD, and AD [28, 71–73]. Two, non-mutually exclusive mechanisms explaining NAcSh atrophy may involve reduced neurite outgrowth and synaptogenesis resulting from reduced expression of *Scn4b*, known to control cell morphology in physiological and pathological conditions [74], and cell death resulting from impaired Ca^{2+} signaling (as discussed above) and abnormal mitochondrial functions.

Architecture of RARβ Binding Motifs

In addition to genomic and functional annotations of potential and bona fide RARβ target genes, our study is also informative about the mode of RARβ control of gene transcription in mouse brain in vivo. In agreement with data obtained from the analysis of mouse embryoid bodies or embryonal carcinoma F9 cells [39], we found that DR0, DR2, DR8, DR5, and IR0 were the most abundant putative RAREs, suggesting a higher preference of RARs binding to these motifs. In complement to those observations, we found DR1 as new frequently occupied motifs in the striatum. Identification of numerous DR8 (for instance, in the *Drd2*, *Gprin3*, *Mapk4*, *Cdh24*, or *Myo5c* genes) confirms that these previously unrecognized elements are a frequent signature of RAR binding in vivo, as first suggested by experiments performed on embryonic stem cells [39]. The functional relevance of a high representation of DR0 (for instance, in *Cbfa2t3*, *Stac2*, *Rora*, *Scarb1*, or *Rnf144b*) has been questioned, as this element was reported to be nonfunctional in vitro when placed in front of minimal promoter, possibly due to steric hindrance in binding of the RAR-RXR heterodimer [39]. However, DR0 elements may contribute to composite DRs, as suggested by Moutier and

colleagues. This possibility is supported in our study by the observation of a frequent coexistence of multiple DRs including DR0, but also DR1, DR3, DR6, and DR10, within individual peaks corresponding to native RARβ DNA binding regions.

We found that 21 % of RARβ binding sites were located intergenically, whereas 24 % of these binding sites were located in the promoter regions with a very high probability (10 % of all RARβ binding sites) of being positioned in the core and proximal promoter. This observation encouraged us to examine the distribution of core elements in the promoters of direct transcriptional targets of RARβ. Intriguingly, for this pool of genes, we did not find any TATA box motifs in core promoters, but only putative Inr, DPE, and BRE motifs, suggesting that RARβ may contribute to differential regulation of distinct core promoter element activities. Such differential regulation has also been reported for negative cofactor 2 (NC2), which may function specifically to activate DPE- and suppress TATA-dependent core promoter activity [75]. Furthermore, DPE core elements may also be regulated by RARβ indirectly. Critical for such regulation could be RARβ interaction with Nuclear Receptor Co-Repressor (N-CoR), which by binding to TAF6 and TAF9 subunits of the TFIID complex [76] could act via DPE elements [77]. The differential association of RARβ with distinct core promoter elements might be an additional "check point" ensuring a high level of transcriptional accuracy and target gene specificity of RARβ transcriptional regulations.

Conclusions

We present here the first genome-wide analysis of RAR binding sites in the brain, and provide a compendium of potential transcriptional targets of RARβ, the major RAR in the striatum and an important regulator of mammalian development—also investigated as a possible tumor suppressor gene. Globally, our analyses point to a strong contribution of RARβ in controlling neurotransmission, energy metabolism, cell morphology and transcription, with a particular involvement of G-protein, cAMP, and calcium signaling (Fig. 6). These regulations may be of relevance for better understanding the pathophysiology of neurodegenerative diseases associated with compromised RA signaling and point to a potential neuroprotective activity of RARβ. Relevance of such findings for HD is further supported by reduction of RARβ expression in R6/2 transgenic mice resulting from partial sequestration of the receptor in HTT aggregates in this animal model of Huntington's disease. Our data pave the way for future functional studies on a gene to gene basis to characterize RARβ regulation of transcriptional target genes in the context of striatal physiology and pathology.

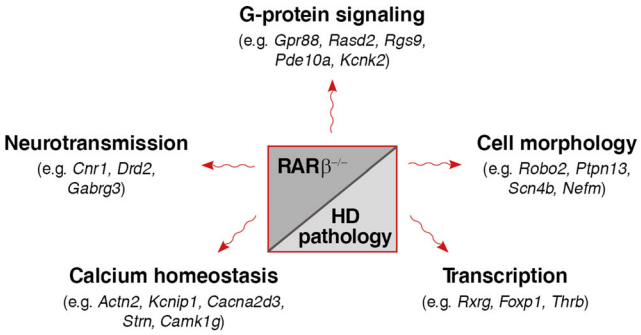

Fig. 6 Scheme of major functions affected by RARβ deficit in the striatum and impaired in Huntington's disease

Materials and Methods

Animals

RARβ knockout (RARβ$^{-/-}$) mice and their WT control littermates were raised on a mixed genetic background (C57BL/6J and 129SvEms/j) as described [78]. To obtain R6/2 transgenic mice animals, WT males on a C57BL/6J x CBA F1 background were crossed with WT females transplanted with ovaries from transgenic HD mice of the R6/2 strain, purchased from Jackson Laboratories (USA). All mice were housed in individually ventilated cages, type "MICE" (Charles River, France) in a 7 am–7 pm light/dark cycle. Food and water were freely available. All experiments were carried out in accordance with the European Community Council Directives of 24 November 1986 (86/609/EEC) and in compliance with the guidelines of CNRS and the French Agricultural and Forestry Ministry (decree 87848).

Chromatin Immunoprecipitation (ChIP) and Sequencing

Chromatin was prepared from four freshly dissected striata enriched for ventral part of striatum. Following cross-linking in 1 % paraformaldehyde (PFA) at room temperature (RT) for 12 min, glycine was added to a final concentration of 0.46 M and incubated for 10 min at RT. Samples were washed in cold PBS/PIC and homogenized in lysis buffer (50 mM Hepes K salt pH 7.9, 1 mM EDTA, 0.13 % Triton X-100, 0.1 % Na-deoxycholate, 0.75 % SDS, 1× PIC). Chromatin was sonicated for 10 min using a Covaris untrasonicator and centrifuged at 16,000 rpm for 5 min. The supernatant was used for subsequent ChIP using antibodies against RARβ, H3K4me3, or GFP (sc-552, Santa Cruz; ab8580, Abcam; ab290, Abcam, respectively). Each 200 µl chromatin sample was diluted 7.5× to a final concentration of 50 mM Hepes K salt pH = 7.9, 140 mM NaCl, 1 mM EDTA, 1 % Triton X-100, 0.1 % Na-deoxycholate, 0.1 % SDS, and 1× PIC. Diluted chromatin was precleared with 40 µl of ProtA beads (Millipore, 16-157) for 45 min at 4 °C, followed by overnight (o/n) incubation with 3 µg of anti-RARβ, -GFP, or -

H3K4me3 antibodies at 4 °C. ProtA-coated beads were added for a 3-h incubation at 4 °C. The beads were washed two times with each of consecutive buffers at 4 °C: IP buffer, buffer A (50 mM Hepes pH 7.9, 500 mM NaCl, 1 mM EDTA, 1 % Triton X-100, 0.1 % Na-deoxycholate, 0.1 % SDS, 1× PIC), buffer B (20 mM Tris pH 8, 1 mM EDTA, 250 mM LiCl, 0.5 % NP40, 0.5 % Na-deoxycholate, 1× PIC), and TE. DNA-protein complexes were eluted from the beads, decrosslinked, and treated with proteinase K for 2 h at 43 °C. DNA fragments were purified using phenol-chloroform, precipitated, and analyzed by qPCR or used for sequencing.

ChIP-seq libraries were prepared using NEXTflex ChIP-Seq Kit (Bio Scientific) following the manufacturer's protocol (V12.10) with some modifications. Briefly, 10 ng of ChIP enriched DNA was end repaired using T4 DNA polymerase, Klenow DNA polymerase, and T4 polynucleotide kinase, size selected, and cleaned-up using Agencourt AMPure XP beads (Beckman). A single "A" nucleotide was added to the 3′ ends of the blunt DNA fragments with the Klenow enzyme. The ends of the DNA fragments were ligated to double-stranded barcoded DNA adapters (NEXTflex ChIP-Seq Barcodes - 6, Bioo Scientific) using T4 DNA ligase. The ligated products were enriched by PCR and cleaned-up using Agencourt AMPure XP beads. Prior to analyses, DNA libraries were checked for quality and quantified using a 2100 Bioanalyzer (Agilent). The libraries were loaded in the flowcell at 8 pM concentration and clusters were generated using the Cbot and sequenced on an Illumina Hiseq2500 system as single-end 50 base reads following Illumina's instructions.

Bioinformatical Analysis

Raw data were analyzed by the Illumina CASAVA 1.8.2 and aligned to the mm9 genome with Bowtie 0.12.7. Peak detection was performed using the MACS 1.4.2 software [79] under settings where an anti-GFP ChIP was used as a negative control. We used a default cutoff p value at $1e^{-05}$, no model build by MACS and a customized shiftsize as 108 bp was set to get an optimizing result. Furthermore, peaks were annotated using GPAT [23] with a window search of 20 kb. For the compatibility of ChIP-seq and transcriptome datasets, we used Homer [35] to annotate the peaks with respect to the coordinates of the beginning and end of Ensembl genes (release 67). A custom JAVA application was used to detect the frequency of DRs, IRs, and ERs in the total RARβ peaks. The same application was also used for the core promoter elements analysis. The core promoter sequences were selected for the transcripts with the closest RARβ peaks. Cluster comparison of ChIP-seq data sets was performed with seqMINER [80]. The statistical significance of transcriptomic changes in the striatum between WT and RARβ$^{-/-}$ animals was confirmed by performing GSEA [81].

Bootstrap Analysis

To verify the statistical significance of the obtained cluster 1, cluster 2, or cluster 3-bound transcript groups in Fig. 4d, we performed bootstrap statistical analyses. In these analyses, we used the total pool of 26,460 Ensembl genes. Next, we randomly selected 6273 genes in the Ensembl total pool. This random selection was then compared with the transcript lists corresponding to different clusters (1045 transcripts for cluster 1, 2595 transcripts for cluster 2, and 2633 transcripts for cluster 3) and the number of transcripts (IDs) belonging to the non-random experimental group was determined. We repeated this process of random selection and gene list crossings 10,000 times and represented the number of IDs and their observed frequencies as histograms (see corresponding Supplementary Fig. S3). For each transcript list, we computed an average (mean) and a standard deviation (sd) of the number of random matches. A z-score is computed as: $z = (\text{mean-expect})/\text{sd}$, where "expect" is the number of expected interest genes. For the three clusters, we obtained a p value lesser than $1.0e^{-16}$. The p value represents the significance of the difference between the randomly found average and the experimental ID numbers.

Immunofluorescence

Brain samples were fresh frozen, and cryosections (14 μm) were collected and postfixed for 10 min in 4 % PFA, followed by washes in PBST (PBS/0.1 % Triton X-100), blocking with 10 % normal goat serum and incubation (o/n at 4 °C) with primary antibodies: anti-RARβ (sc-552), anti-hHTT recognizing amino acids 50–64 of human Huntingtin (2B4). Secondary antibodies conjugated with Alexa 555 and Alexa 488 fluorophores and DAPI were used for detection. For all experiments, four animals of each genotype were analyzed.

Confocal Microscopy

Images were obtained using a SP8 Leica inverted-based microscope with ×63 objective and with zoom factor 2.5. To perform quantitative fluorescent measurements of RARβ expression level, DPSS561 laser power was kept constant for all acquisitions (each Z-stack in WT and transgenic brain sections). Quantitative fluorescence measurements and colocalization studies were performed using the Imaris software by creating the mask of nuclei and mask of HTT aggregates, which were next used to calculate the mean intensity of RARβ signal in corresponding regions. Quantification was carried out on 20–40 cells/animal for each striatal subregion. Data were analyzed using two-way ANOVA with genotype and striatal region as two independent variables or by two-tailed, unpaired t test for post-hoc analyses or two group comparisons.

Transcriptome (DNA Microarray) Analysis

Dissection of the Nucleus Accumbens and RNA Extraction

Behaviorally naive RARβ$^{-/-}$ mice ($n=6$) and their WT littermates ($n=5$) were sacrificed by cervical dislocation at the age of 4 months. Brains were fresh frozen in Shandon Cryomatrix (Thermo Scientific) and kept at −80 °C until use. NAcSh was dissected bilaterally under a stereomicroscope (Leica), from three subsequent 300 μm cryosections using 0.5 mm corer. RNA was isolated using the RNeasy Micro Kit (Qiagen) and kept at −80 °C for further analysis.

Hybridization on Microarrays and Analysis

The quality of RNA was determined by capillary electrophoresis in a 2100 Bioanalyzer (Agilent). RNA was next used to synthesize sense-strand cDNA, which was further labeled, fragmented, and hybridized on Affymetrix GeneChip Mouse Gene 1.0 ST arrays. Raw microarray data were normalized using a log scale robust multi-array analysis (RMA) [82, 83] in the Partek Genomics Suite 6.5 software and subsequently subjected to principal components analysis (PCA) in order to assess samples distribution. Only transcripts which were found to be significantly expressed (hybridization signal value above 5.76—30th percentile of all expression values) were retained for further analyses. Differences in gene expression were evaluated for average intensity signal for WT and RARβ$^{-/-}$ groups and expressed as $\log_2$ of the ratio of RARβ$^{-/-}$ to WT value (fold change, FC). The statistical significance of gene expression was assigned using two-tailed, unpaired *t* test. Genes were considered to be significantly regulated if the FC of gene expression was $0.8 \geq FC \geq 1.2$ at p value <0.05 (FDR = 0.2, Benjamini and Hochberg method). Using another statistical method FCROS [84], we found almost the same selection (>95 % of common IDs) with smaller error (10 %). Stringent threshold level (*t* test threshold = 0.01, FDR = 0.09) was used for the volcano plot and for gene validation. Gene functional annotation was performed using Ingenuity (*t* test threshold = 0.05). Additional analyses of an overlap between HD-deregulated genes reported in the literature and RARβ target genes were also performed by analyses of hypergeometric distribution using phyper from R software library.

Quantitative RT-PCR

Quantitative RT-PCR (qPCR) was performed on RNA samples used for microarray hybridization and from an additional group of four mice/genotype. cDNA was synthesized using QuantiTect Reverse Transcription Kit (Qiagen) according to the manufacturer's protocol. The real-time qPCR reactions were performed in a LightCycler 480 (Roche) using gene-specific primers (Supplementary Table S8) and QuantiFast SYBR Green PCR Kit (Qiagen). The amount of transcripts was evaluated relatively to the expression level of the housekeeping gene acidic ribosomal phosphoprotein P0 (Rplp0 or 36B4). Statistical analysis was performed using two-tailed, unpaired *t* test.

Data Access

The data have been submitted to the NCBI Gene Expression Omnibus (GEO) (http://www.ncbi.nlm.nih.gov/geo/) under accession No. GSE67829, and GSE67761.

Acknowledgments This work was supported by a grant from the Agence Nationale de la Recherche (ANR grant ReSiNEs, ANR-11-BSV2-0003) to P.D. and by an institutional grant (LabEx ANR-10-LABX-0030-INRT) under the frame program Investissements d'Avenir labeled ANR-10-IDEX-0002-02. A.N-C was supported by ReSiNEs and by LabEx INRT funds, and A.P-D. by a PhD fellowship from INRT funds. A.K. was supported by fellowships from the French government (cotutelle), financement relais du Collège Doctoral Européen, and ANR (grant Neuroprotect; ANR-07-PNRA-022-04 to W.K.). We thank C. Thibault-Carpentier, B. Jost, I. Martianov, A. Oravecz, and K. Merienne, for helpful discussions concerning ChIP and transcriptomic analyses; V. Alunni and S. Vicaire from the IGBMC Microarray and High-Throughput Sequencing Platform for processing Affymetrix chips and Illumina libraries, respectively. The Platform is supported by the France Génomique National infrastructure, funded as part of the Investissements d'Avenir program ANR-10-INBS-09. We thank also Y. Trottier and C. Weber for advice on R6/2 line maintenance, P. Kessler from the IGBMC Imaging Platform for assistance in image acquisition and analyses, and V. Fraulob, B. Schuhbaur and J. Sikora for technical assistance.

Compliance with Ethical Standards

Disclosure Declaration The authors have no situation of conflict of interest to declare.

References

1. Kane MA, Chen N, Sparks S, Napoli JL (2005) Quantification of endogenous retinoic acid in limited biological samples by LC/MS/MS. Biochem J 388(Pt 1):363–369
2. Krezel W, Kastner P, Chambon P (1999) Differential expression of retinoid receptors in the adult mouse central nervous system. Neuroscience 89(4):1291–1300
3. Zetterstrom RH, Simon A, Giacobini MM, Eriksson U, Olson L (1994) Localization of cellular retinoid-binding proteins suggests specific roles for retinoids in the adult central nervous system. Neuroscience 62(3):899–918
4. Krezel W, Ghyselinck N, Samad TA, Dupe V, Kastner P, Borrelli E, Chambon P (1998) Impaired locomotion and dopamine signaling in retinoid receptor mutant mice. Science 279(5352):863–867
5. Krzyzosiak A, Szyszka-Niagolov M, Wietrzych M, Gobaille S, Muramatsu S, Krezel W (2010) Retinoid x receptor gamma control of affective behaviors involves dopaminergic signaling in mice. Neuron 66(6):908–920
6. Liao WL, Tsai HC, Wang HF, Chang J, Lu KM, Wu HL, Lee YC, Tsai TF et al (2008) Modular patterning of structure and function of

the striatum by retinoid receptor signaling. Proc Natl Acad Sci U S A 105(18):6765–6770
7. Rataj-Baniowska M, Niewiadomska-Cimicka A, Paschaki M, Szyszka-Niagolov M, Carramolino L, Torres M, Dolle P, Krezel W (2015) Retinoic acid receptor beta controls development of striatonigral projection neurons through FGF-dependent and Meis1-dependent mechanisms. J Neurosci 35(43):14467–14475
8. Wietrzych-Schindler M, Szyszka-Niagolov M, Ohta K, Endo Y, Perez E, de Lera AR, Chambon P, Krezel W (2011) Retinoid x receptor gamma is implicated in docosahexaenoic acid modulation of despair behaviors and working memory in mice. Biol Psychiatry 69(8):788–794
9. Lane MA, Bailey SJ (2005) Role of retinoid signalling in the adult brain. Prog Neurobiol 75(4):275–293
10. Balmer JE, Blomhoff R (2002) Gene expression regulation by retinoic acid. J Lipid Res 43(11):1773–1808
11. de The H, Vivanco-Ruiz MM, Tiollais P, Stunnenberg H, Dejean A (1990) Identification of a retinoic acid responsive element in the retinoic acid receptor beta gene. Nature 343(6254):177–180
12. Sucov HM, Murakami KK, Evans RM (1990) Characterization of an autoregulated response element in the mouse retinoic acid receptor type beta gene. Proc Natl Acad Sci U S A 87(14):5392–5396
13. Samad TA, Krezel W, Chambon P, Borrelli E (1997) Regulation of dopaminergic pathways by retinoids: activation of the D2 receptor promoter by members of the retinoic acid receptor-retinoid X receptor family. Proc Natl Acad Sci U S A 94(26):14349–14354
14. Crittenden JR, Graybiel AM (2011) Basal ganglia disorders associated with imbalances in the striatal striosome and matrix compartments. Front Neuroanat 5:59
15. Galter D, Buervenich S, Carmine A, Anvret M, Olson L (2003) ALDH1 mRNA: presence in human dopamine neurons and decreases in substantia nigra in Parkinson's disease and in the ventral tegmental area in schizophrenia. Neurobiol Dis 14(3):637–647
16. Corcoran JP, So PL, Maden M (2004) Disruption of the retinoid signalling pathway causes a deposition of amyloid beta in the adult rat brain. Eur J Neurosci 20(4):896–902
17. Rinaldi P, Polidori MC, Metastasio A, Mariani E, Mattioli P, Cherubini A, Catani M, Cecchetti R et al (2003) Plasma antioxidants are similarly depleted in mild cognitive impairment and in Alzheimer's disease. Neurobiol Aging 24(7):915–919
18. Goncalves MB, Clarke E, Hobbs C, Malmqvist T, Deacon R, Jack J, Corcoran JP (2013) Amyloid beta inhibits retinoic acid synthesis exacerbating Alzheimer disease pathology which can be attenuated by an retinoic acid receptor alpha agonist. Eur J Neurosci 37(7):1182–1192
19. Fitzmaurice AG, Rhodes SL, Lulla A, Murphy NP, Lam HA, O'Donnell KC, Barnhill L, Casida JE et al (2013) Aldehyde dehydrogenase inhibition as a pathogenic mechanism in Parkinson disease. Proc Natl Acad Sci U S A 110(2):636–641
20. Hodges A, Strand AD, Aragaki AK, Kuhn A, Sengstag T, Hughes G, Elliston LA, Hartog C et al (2006) Regional and cellular gene expression changes in human Huntington's disease brain. Hum Mol Genet 15(6):965–977
21. Luthi-Carter R, Strand A, Peters NL, Solano SM, Hollingsworth ZR, Menon AS, Frey AS, Spektor BS et al (2000) Decreased expression of striatal signaling genes in a mouse model of Huntington's disease. Hum Mol Genet 9(9):1259–1271
22. Delacroix L, Moutier E, Altobelli G, Legras S, Poch O, Choukrallah MA, Bertin I, Jost B et al (2010) Cell-specific interaction of retinoic acid receptors with target genes in mouse embryonic fibroblasts and embryonic stem cells. Mol Cell Biol 30(1):231–244
23. Krebs A, Frontini M, Tora L (2008) GPAT: retrieval of genomic annotation from large genomic position datasets. BMC Bioinformatics 9:533
24. da Huang W, Sherman BT, Lempicki RA (2009) Systematic and integrative analysis of large gene lists using DAVID bioinformatics resources. Nat Protoc 4(1):44–57
25. McLean CY, Bristor D, Hiller M, Clarke SL, Schaar BT, Lowe CB, Wenger AM, Bejerano G (2010) GREAT improves functional interpretation of cis-regulatory regions. Nat Biotechnol 28(5):495–501
26. Mahony S, Mazzoni EO, McCuine S, Young RA, Wichterle H, Gifford DK (2011) Ligand-dependent dynamics of retinoic acid receptor binding during early neurogenesis. Genome Biol 12(1):R2
27. Mendoza-Parra MA, Walia M, Sankar M, Gronemeyer H (2011) Dissecting the retinoid-induced differentiation of F9 embryonal stem cells by integrative genomics. Mol Syst Biol 7:538
28. van den Bogaard SJ, Dumas EM, Acharya TP, Johnson H, Langbehn DR, Scahill RI, Tabrizi SJ, van Buchem MA et al (2011) Early atrophy of pallidum and accumbens nucleus in Huntington's disease. J Neurol 258(3):412–420
29. Vonsattel JP, Myers RH, Stevens TJ, Ferrante RJ, Bird ED, Richardson EP Jr (1985) Neuropathological classification of Huntington's disease. J Neuropathol Exp Neurol 44(6):559–577
30. Bi J, Hu X, Loh HH, Wei LN (2001) Regulation of mouse kappa opioid receptor gene expression by retinoids. J Neurosci 21(5):1590–1599
31. Desplats PA, Kass KE, Gilmartin T, Stanwood GD, Woodward EL, Head SR, Sutcliffe JG, Thomas EA (2006) Selective deficits in the expression of striatal-enriched mRNAs in Huntington's disease. J Neurochem 96(3):743–757
32. Zetterstrom RH, Lindqvist E, Mata de Urquiza A, Tomac A, Eriksson U, Perlmann T, Olson L (1999) Role of retinoids in the CNS: differential expression of retinoid binding proteins and receptors and evidence for presence of retinoic acid. Eur J Neurosci 11(2):407–416
33. Lein ES, Hawrylycz MJ, Ao N, Ayres M, Bensinger A, Bernard A, Boe AF, Boguski MS et al (2007) Genome-wide atlas of gene expression in the adult mouse brain. Nature 445(7124):168–176
34. Mangiarini L, Sathasivam K, Seller M, Cozens B, Harper A, Hetherington C, Lawton M, Trottier Y et al (1996) Exon 1 of the HD gene with an expanded CAG repeat is sufficient to cause a progressive neurological phenotype in transgenic mice. Cell 87(3):493–506
35. Heinz S, Benner C, Spann N, Bertolino E, Lin YC, Laslo P, Cheng JX, Murre C et al (2010) Simple combinations of lineage-determining transcription factors prime cis-regulatory elements required for macrophage and B cell identities. Mol Cell 38(4):576–589
36. Mangelsdorf DJ, Umesono K, Kliewer SA, Borgmeyer U, Ong ES, Evans RM (1991) A direct repeat in the cellular retinol-binding protein type II gene confers differential regulation by RXR and RAR. Cell 66(3):555–561
37. Nakshatri H, Chambon P (1994) The directly repeated RG(G/T)TCA motifs of the rat and mouse cellular retinol-binding protein II genes are promiscuous binding sites for RAR, RXR, HNF-4, and ARP-1 homo- and heterodimers. J Biol Chem 269(2):890–902
38. Bastien J, Rochette-Egly C (2004) Nuclear retinoid receptors and the transcription of retinoid-target genes. Gene 328:1–16
39. Moutier E, Ye T, Choukrallah MA, Urban S, Osz J, Chatagnon A, Delacroix L, Langer D et al (2012) Retinoic acid receptors recognize the mouse genome through binding elements with diverse spacing and topology. J Biol Chem 287(31):26328–26341
40. Thomas-Chollier M, Herrmann C, Defrance M, Sand O, Thieffry D, van Helden J (2012) RSAT peak-motifs: motif analysis in full-size ChIP-seq datasets. Nucleic Acids Res 40(4), e31
41. Juven-Gershon T, Kadonaga JT (2010) Regulation of gene expression via the core promoter and the basal transcriptional machinery. Dev Biol 339(2):225–229

42. Mukhopadhyay B, Liu J, Osei-Hyiaman D, Godlewski G, Mukhopadhyay P, Wang L, Jeong WI, Gao B et al (2010) Transcriptional regulation of cannabinoid receptor-1 expression in the liver by retinoic acid acting via retinoic acid receptor-gamma. J Biol Chem 285(25):19002–19011
43. Iniguez MA, Morte B, Rodriguez-Pena A, Munoz A, Gerendasy D, Sutcliffe JG, Bernal J (1994) Characterization of the promoter region and flanking sequences of the neuron-specific gene RC3 (neurogranin). Brain Res Mol Brain Res 27(2):205–214
44. Everitt BJ, Robbins TW (2013) From the ventral to the dorsal striatum: devolving views of their roles in drug addiction. Neurosci Biobehav Rev 37(9 Pt A):1946–1954
45. Ramirez AD, Smith SM (2014) Regulation of dopamine signaling in the striatum by phosphodiesterase inhibitors: novel therapeutics to treat neurological and psychiatric disorders. Cent Nerv Syst Agents Med Chem 14(2):72–82
46. Martin AB, Fernandez-Espejo E, Ferrer B, Gorriti MA, Bilbao A, Navarro M, Rodriguez de Fonseca F, Moratalla R (2008) Expression and function of CB1 receptor in the rat striatum: localization and effects on D1 and D2 dopamine receptor-mediated motor behaviors. Neuropsychopharmacology 33(7):1667–1679
47. Hoppa MB, Lana B, Margas W, Dolphin AC, Ryan TA (2012) Alpha2delta expression sets presynaptic calcium channel abundance and release probability. Nature 486(7401):122–125
48. Benoist M, Gaillard S, Castets F (2006) The striatin family: a new signaling platform in dendritic spines. J Physiol Paris 99(2–3):146–153
49. Huang KP, Huang FL, Jager T, Li J, Reymann KG, Balschun D (2004) Neurogranin/RC3 enhances long-term potentiation and learning by promoting calcium-mediated signaling. J Neurosci 24(47):10660–10669
50. Kamei Y, Xu L, Heinzel T, Torchia J, Kurokawa R, Gloss B, Lin SC, Heyman RA et al (1996) A CBP integrator complex mediates transcriptional activation and AP-1 inhibition by nuclear receptors. Cell 85(3):403–414
51. Kurokawa R, Soderstrom M, Horlein A, Halachmi S, Brown M, Rosenfeld MG, Glass CK (1995) Polarity-specific activities of retinoic acid receptors determined by a co-repressor. Nature 377(6548):451–454
52. Steffan JS, Kazantsev A, Spasic-Boskovic O, Greenwald M, Zhu YZ, Gohler H, Wanker EE, Bates GP et al (2000) The Huntington's disease protein interacts with p53 and CREB-binding protein and represses transcription. Proc Natl Acad Sci U S A 97(12):6763–6768
53. Boutell JM, Thomas P, Neal JW, Weston VJ, Duce J, Harper PS, Jones AL (1999) Aberrant interactions of transcriptional repressor proteins with the Huntington's disease gene product, huntingtin. Hum Mol Genet 8(9):1647–1655
54. Mey J, McCaffery P (2004) Retinoic acid signaling in the nervous system of adult vertebrates. Neuroscientist 10(5):409–421
55. Chaturvedi RK, Flint Beal M (2013) Mitochondrial diseases of the brain. Free Radic Biol Med 63:1–29
56. Cha JH (2000) Transcriptional dysregulation in Huntington's disease. Trends Neurosci 23(9):387–392
57. Zhai W, Jeong H, Cui L, Krainc D, Tjian R (2005) In vitro analysis of huntingtin-mediated transcriptional repression reveals multiple transcription factor targets. Cell 123(7):1241–1253
58. Shimohata T, Nakajima T, Yamada M, Uchida C, Onodera O, Naruse S, Kimura T, Koide R et al (2000) Expanded polyglutamine stretches interact with TAFII130, interfering with CREB-dependent transcription. Nat Genet 26(1):29–36
59. Nucifora FC Jr, Sasaki M, Peters MF, Huang H, Cooper JK, Yamada M, Takahashi H, Tsuji S et al (2001) Interference by huntingtin and atrophin-1 with cbp-mediated transcription leading to cellular toxicity. Science 291(5512):2423–2428
60. Dunah AW, Jeong H, Griffin A, Kim YM, Standaert DG, Hersch SM, Mouradian MM, Young AB et al (2002) Sp1 and TAFII130 transcriptional activity disrupted in early Huntington's disease. Science 296(5576):2238–2243
61. Li SH, Cheng AL, Zhou H, Lam S, Rao M, Li H, Li XJ (2002) Interaction of Huntington disease protein with transcriptional activator Sp1. Mol Cell Biol 22(5):1277–1287
62. Schaffar G, Breuer P, Boteva R, Behrends C, Tzvetkov N, Strippel N, Sakahira H, Siegers K et al (2004) Cellular toxicity of polyglutamine expansion proteins: mechanism of transcription factor deactivation. Mol Cell 15(1):95–105
63. Strand AD, Aragaki AK, Shaw D, Bird T, Holton J, Turner C, Tapscott SJ, Tabrizi SJ et al (2005) Gene expression in Huntington's disease skeletal muscle: a potential biomarker. Hum Mol Genet 14(13):1863–1876
64. Kuhn A, Goldstein DR, Hodges A, Strand AD, Sengstag T, Kooperberg C, Becanovic K, Pouladi MA et al (2007) Mutant huntingtin's effects on striatal gene expression in mice recapitulate changes observed in human Huntington's disease brain and do not differ with mutant huntingtin length or wild-type huntingtin dosage. Hum Mol Genet 16(15):1845–1861
65. Chaturvedi RK, Adhihetty P, Shukla S, Hennessy T, Calingasan N, Yang L, Starkov A, Kiaei M et al (2009) Impaired PGC-1alpha function in muscle in Huntington's disease. Hum Mol Genet 18(16):3048–3065
66. Tang B, Becanovic K, Desplats PA, Spencer B, Hill AM, Connolly C, Masliah E, Leavitt BR et al (2012) Forkhead box protein p1 is a transcriptional repressor of immune signaling in the CNS: implications for transcriptional dysregulation in Huntington disease. Hum Mol Genet 21(14):3097–3111
67. Benayoun BA, Pollina EA, Ucar D, Mahmoudi S, Karra K, Wong ED, Devarajan K, Daugherty AC et al (2014) H3K4me3 breadth is linked to cell identity and transcriptional consistency. Cell 158(3):673–688
68. Ujike H, Takaki M, Nakata K, Tanaka Y, Takeda T, Kodama M, Fujiwara Y, Sakai A et al (2002) CNR1, central cannabinoid receptor gene, associated with susceptibility to hebephrenic schizophrenia. Mol Psychiatry 7(5):515–518
69. Catapano LA, Manji HK (2007) G protein-coupled receptors in major psychiatric disorders. Biochim Biophys Acta 1768(4):976–993
70. Moreno JL, Holloway T, Gonzalez-Maeso J (2013) G protein-coupled receptor heterocomplexes in neuropsychiatric disorders. Prog Mol Biol Transl Sci 117:187–205
71. Hanganu A, Bedetti C, Degroot C, Mejia-Constain B, Lafontaine AL, Soland V, Chouinard S, Bruneau MA et al (2014) Mild cognitive impairment is linked with faster rate of cortical thinning in patients with Parkinson's disease longitudinally. Brain 137(Pt 4):1120–1129
72. Mavridis I, Boviatsis E, Anagnostopoulou S (2011) The human nucleus accumbens suffers parkinsonism-related shrinkage: a novel finding. Surg Radiol Anat 33(7):595–599
73. Pievani M, Bocchetta M, Boccardi M, Cavedo E, Bonetti M, Thompson PM, Frisoni GB (2013) Striatal morphology in early-onset and late-onset Alzheimer's disease: a preliminary study. Neurobiol Aging 34(7):1728–1739
74. Oyama F, Miyazaki H, Sakamoto N, Becquet C, Machida Y, Kaneko K, Uchikawa C, Suzuki T et al (2006) Sodium channel beta4 subunit: down-regulation and possible involvement in neuritic degeneration in Huntington's disease transgenic mice. J Neurochem 98(2):518–529
75. Willy PJ, Kobayashi R, Kadonaga JT (2000) A basal transcription factor that activates or represses transcription. Science 290(5493):982–985
76. Muscat GE, Burke LJ, Downes M (1998) The corepressor N-CoR and its variants RIP13a and RIP13Delta1 directly interact with the

basal transcription factors TFIIB, TAFII32 and TAFII70. Nucleic Acids Res 26(12):2899–2907

77. Burke TW, Kadonaga JT (1997) The downstream core promoter element, DPE, is conserved from *Drosophila* to humans and is recognized by TAFII60 of *Drosophila*. Genes Dev 11(22):3020–3031
78. Ghyselinck NB, Dupé V, Dierich A, Messaddeq N, Garnier JM, Rochette-Egly C, Chambon P, Mark M (1997) Role of the retinoic acid receptor beta (RARbeta) during mouse development. Int J Dev Biol 41(3):425–447
79. Zhang Y, Liu T, Meyer CA, Eeckhoute J, Johnson DS, Bernstein BE, Nusbaum C, Myers RM et al (2008) Model-based analysis of ChIP-Seq (MACS). Genome Biol 9(9):R137
80. Ye T, Krebs AR, Choukrallah MA, Keime C, Plewniak F, Davidson I, Tora L (2011) seqMINER: an integrated ChIP-seq data interpretation platform. Nucleic Acids Res 39(6):e35
81. Subramanian A, Tamayo P, Mootha VK, Mukherjee S, Ebert BL, Gillette MA, Paulovich A, Pomeroy SL et al (2005) Gene set enrichment analysis: a knowledge-based approach for interpreting genome-wide expression profiles. Proc Natl Acad Sci U S A 102(43):15545–15550
82. Bolstad BM, Irizarry RA, Astrand M, Speed TP (2003) A comparison of normalization methods for high density oligonucleotide array data based on variance and bias. Bioinformatics 19(2):185–193
83. Irizarry RA, Hobbs B, Collin F, Beazer-Barclay YD, Antonellis KJ, Scherf U, Speed TP (2003) Exploration, normalization, and summaries of high density oligonucleotide array probe level data. Biostatistics 4(2):249–264
84. Dembele D, Kastner P (2014) Fold change rank ordering statistics: a new method for detecting differentially expressed genes. BMC Bioinformatics 15:14